Supporting Information

TITLE: Discovery and biological characterization of PRMT5:MEP50 protein:protein interaction inhibitors

AUTHORS: Andrew M. Asberry[1,2,‡], Xinpei Cai[3,‡], Xuehong Deng[1,‡], Ulises Santiago[4,‡], Sheng Liu[5,6], Hunter S. Sims[3], Weida Liang[3], Xueyong Xu[7], Jun Wan[5,6,8] , Wen Jiang [7,9], Carlos J. Camacho[4]*, Mingji Dai[3,9,10]*, and Chang-Deng Hu[1,9*†]

AFFILIATIONS

[1] Department of Medicinal Chemistry and Molecular Pharmacology, Purdue University, West Lafayette, IN, 47907, USA.
[2] Purdue University Interdisciplinary Life Sciences Graduate Program, Purdue University, West Lafayette, IN, 47907, USA.
[3] Department of Chemistry, Purdue University, West Lafayette, IN, 47907, USA
[4] Department of Computational and Systems Biology, University of Pittsburgh, Pittsburgh, PA, 15260, USA
[5] Department of Medical and Molecular Genetics, Indiana University School of Medicine, Indianapolis, IN, 46202, USA.
[6] The Indiana University Melvin and Bren Simon Cancer Center, Indiana University, Indianapolis, IN, 46202, USA.
[7] Department of Biological Sciences, Purdue University, 240 S Martin Jischke Drive, West Lafayette, IN 47907, USA
[8] The Center for Computational Biology and Bioinformatics, Indiana University School of Medicine, Indianapolis, IN, 46202, USA.
[9] Purdue University Center for Cancer Research, Purdue University, West Lafayette, IN, 47907, USA.
[10] Department of Chemistry, Emory University, Atlanta, GA, 30322, USA.
‡ Authors contributed equally to this work
† Deceased on September 1, 2022

EMAIL ADDRESS

Chang-Deng Hu, MD, Ph.D.: hu1@purdue.edu
Mingji Dai, Ph.D.: mingji.dai@emory.edu
Carlos Camacho, Ph.D.: ccamacho@pitt.edu

CONTENTS OF SUPPORTING INFORMATION:

Supporting Information.pdf: Fig. S1-S6 and compound identity and purity (NMR/HPLC)
SI_Spreadsheet.xlsx: Biological reagents used
SI_SMILES.csv: Compound SMILES format and biological data
4gqb.MP8.pdb: Molecular docking 3D model

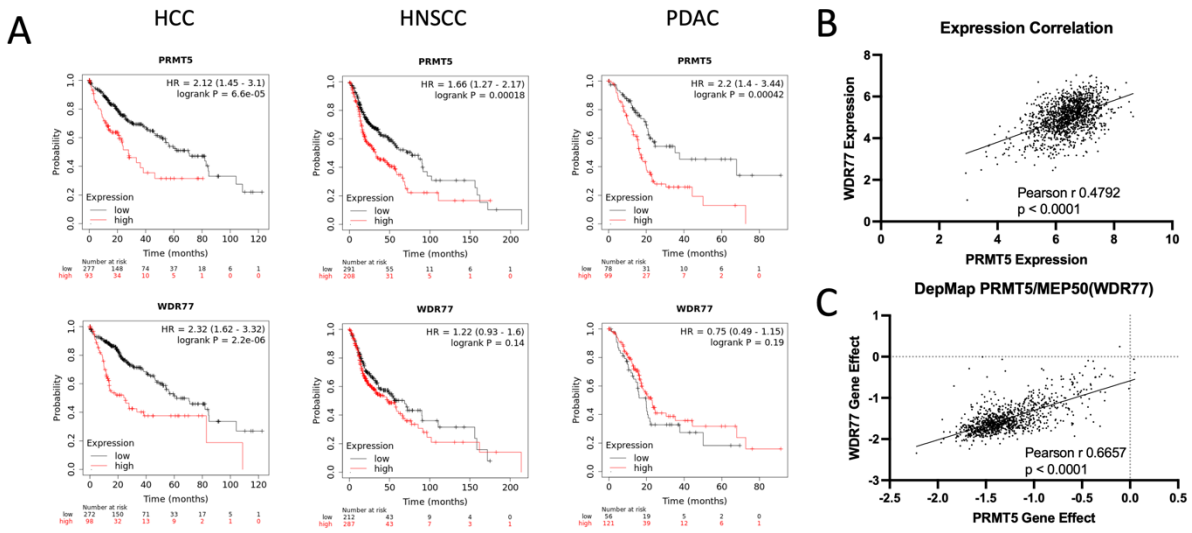

Figure S1. PRMT5 and MEP50 Expression is Positively Correlated and Indicates Poor Prognosis. (A) Overall survival curve based on high/low stratified PRMT5 (top row) and MEP50/WDR77 (bottom row) expression in hepatocellular carcinoma (HCC), head/neck squamous cell carcinoma (HNSCC), and pancreatic ductal adenocarcinoma (PDAC) from GEO/EGA/TCGA database (B) Expression correlation of PRMT5 and MEP50/WDR77 in >1300 cell lines (Broad Institute) (C) Gene Dependency (lethality of gene loss) correlation between PRMT5 and MEP50/WDR77 genes in >1300 cell lines (Broad Institute)

A

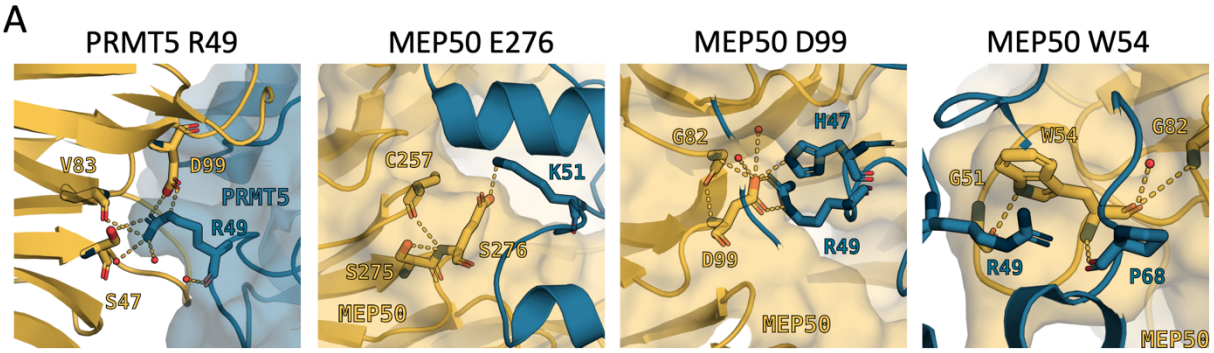

B

PRMT5 Residues

energy (kcal/mol)	index	AA.
-9.709	166	ASP
-9.471	51	LYS
-7.95	161	GLU
-7.524	49	ARG
-5.097	62	ARG
-4.026	167	ILE
-3.36	168	ILE
-2.972	24	PRO
-2.578	68	ARG
-2.549	85	LYS
-2.28	50	PHE

C

MEP50 Residues

energy (kcal/mol)	index	AA.
-9.442	201	LYS
-8.959	276	GLU
-8.414	99	ASP
-7.003	191	ARG
-6.21	298	ASP
-4.511	52	ARG
-4.246	126	ASP
-3.992	32	GLU
-3.58	54	TRP
-2.659	164	ARG
-2.601	49	LEU

D

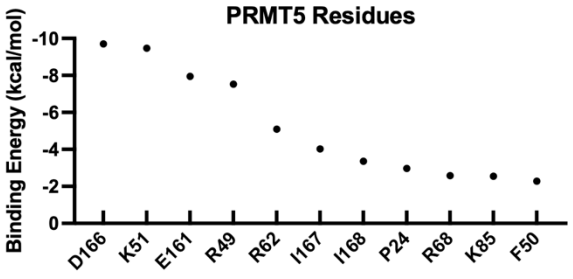

E

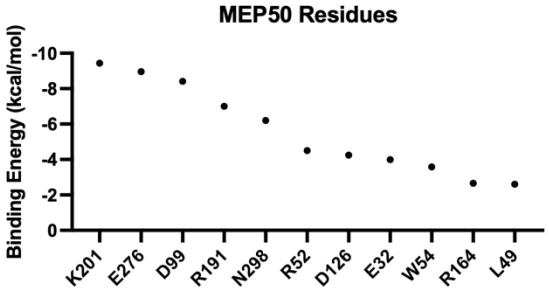

Figure S2. PRMT5 and MEP50 Electrostatic Interactions and Binding Energy. (A) All ≤4 angstrom contacts for residues PRMT5 R49 (left), MEP50 E276 (middle left), MEP50 D99 (middle right), and MEP50 W54 (right). Waters in crystal structure 4GQB shown as red spheres. (B,C) Predicted binding energy for top 11 residues mediating PRMT5:MEP50 protein:protein interaction for PRMT5 (B) and MEP50 (C). (D,E) Graphical portrayal ranked order for binding energy listed in (B,C).

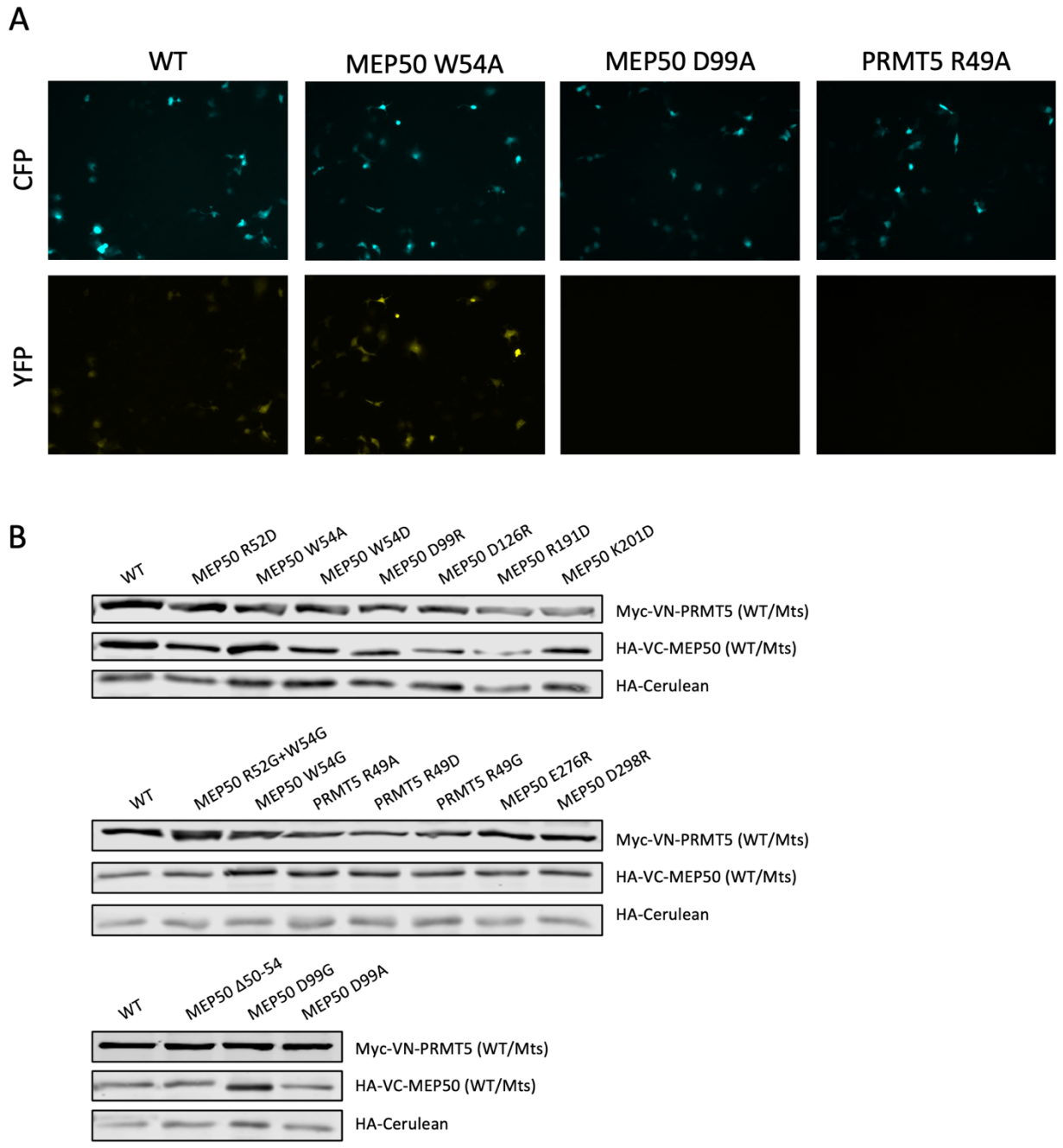

Figure S3. PRMT5 and MEP50 Mutants in BiFC Screen. (A) Representative Cerulean fluorescent protein (CFP) and Venus / Yellow fluorescent protein (YFP) images from BiFC mutant interaction experiment acquired at 10X magnification. (B) Western blots showing Myc-tagged PRMT5(TIM) (Myc-VN-PRMT5) wild type (WT) or Mutants (Mts), HA-tagged MEP50 (HA-VC-MEP50) wild type (WT) or mutants (Mts), HA-tagged Cerulean (HA-Cerulean) fusion protein expression via western blot

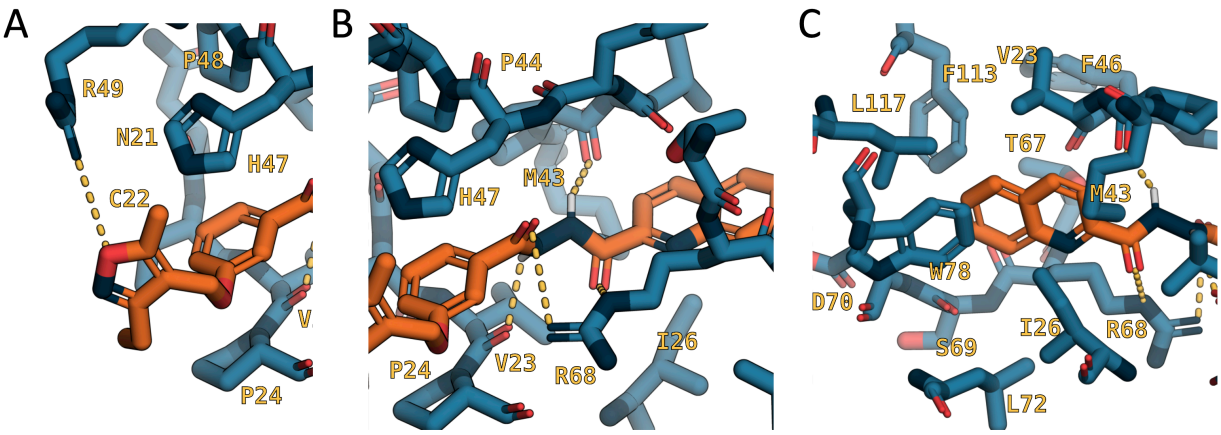

Figure S4. Detailed Predicted Binding Mode of Compound 17. (A) Orientation and interaction of isoxazole ring with PRMT5 R49. (B) Orientation and interactions of linker with PRMT5 M43, V23, and R68. (C) Orientation of quinoline ring in pocket of PRMT5.

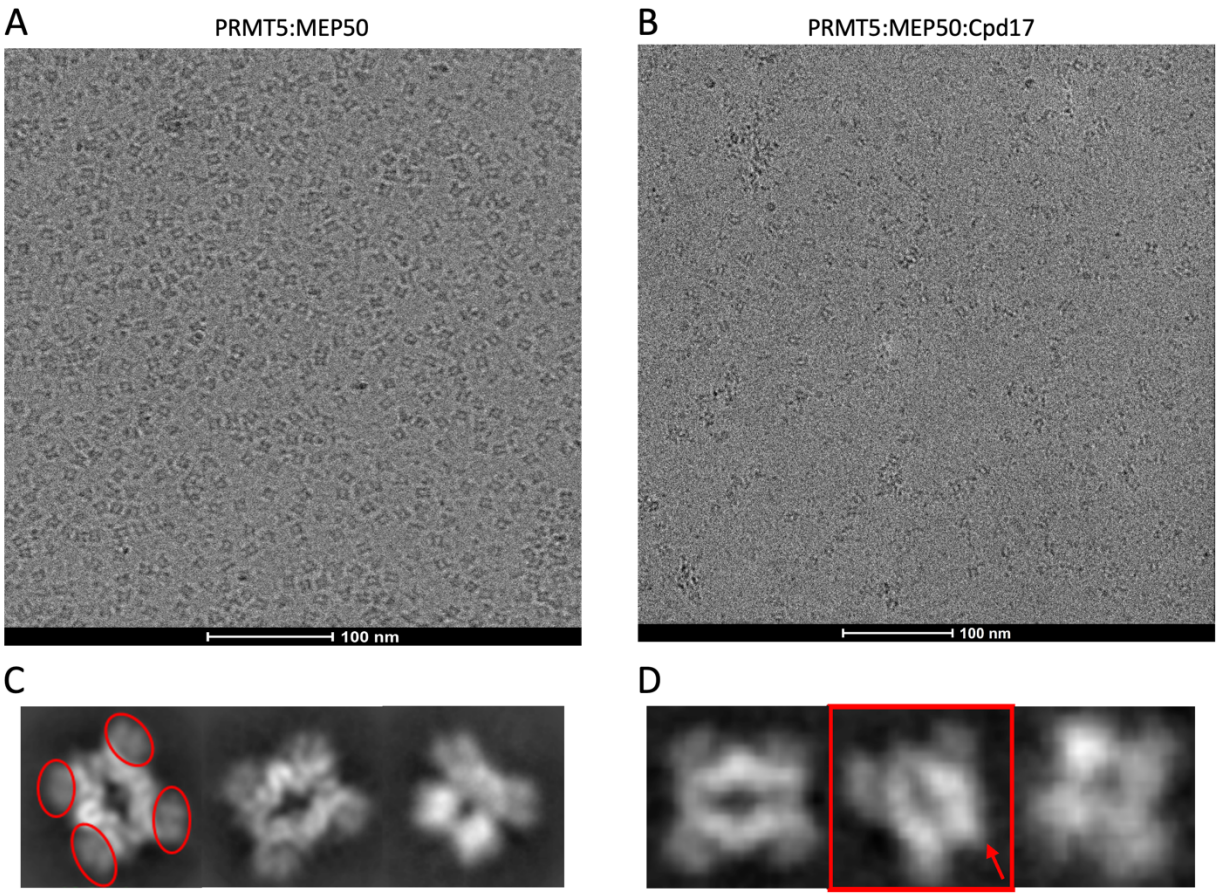

Figure S5. Cryo-EM micrograph indicates Compound 17 displaces MEP50 subunit(s). (A, B) Representative cryo-EM micrograph of PRMT5/MEP50 and PRMT5/MEP50/Cpd ***17***, respectively. Scale bars, 100 nm. (C, D) 2D class averages of PRMT5/MEP50 and PRMT5/MEP50/Cpd ***17***, respectively. Four copies of MEP50 represented in red circles in (C) decorate the outer surface of the molecule. Smaller particles and aggregates can be observed in (B). 2D class average highlighted in red square in (D) suggests one MEP50 is displaced (indicated by red arrow) in the presence of Cpd ***17*** .

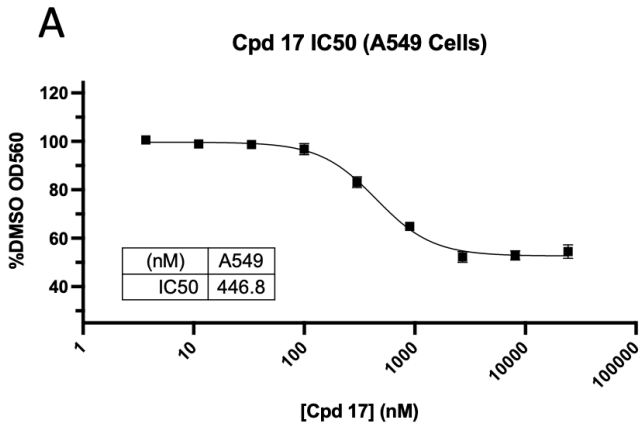

Figure S6. Compound 17 IC_{50} in A549 cancer cell line. (A) IC50 Curve for A549 (non-small cell lung cancer (NSCLC)) cell line treated with Cpd ***17*** for 72 h.

NMR Spectra

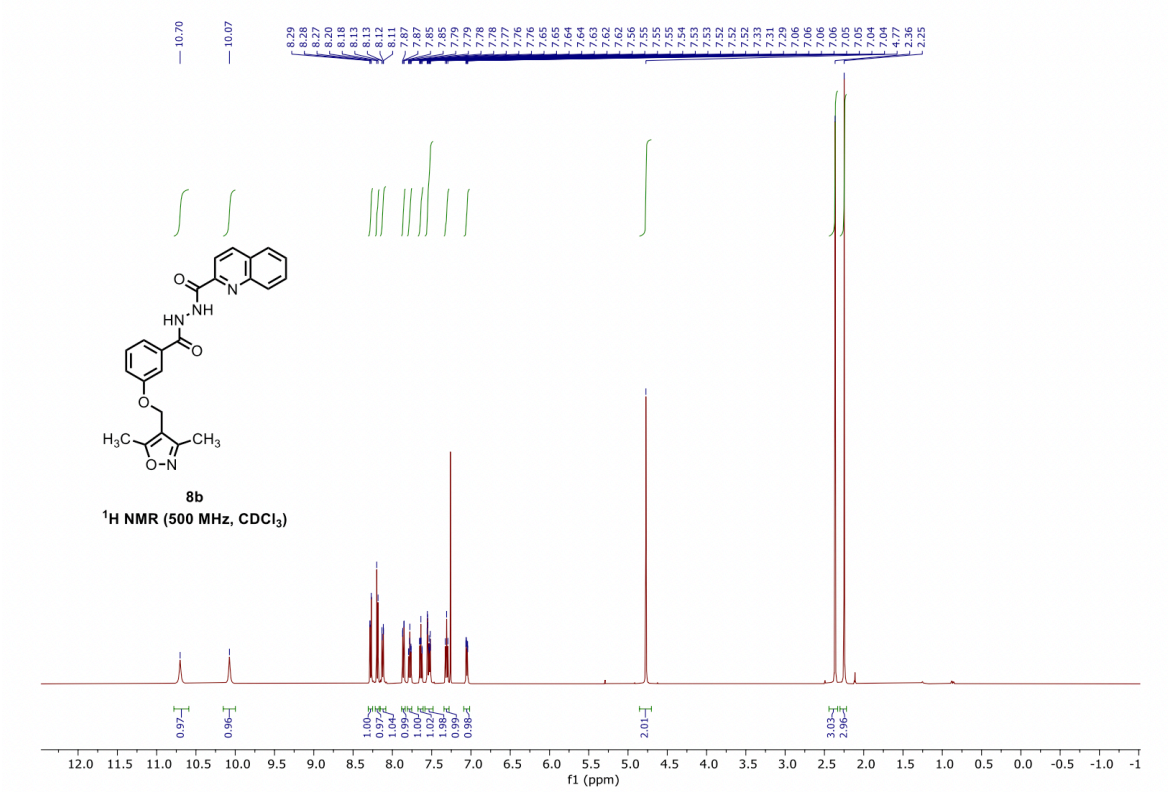

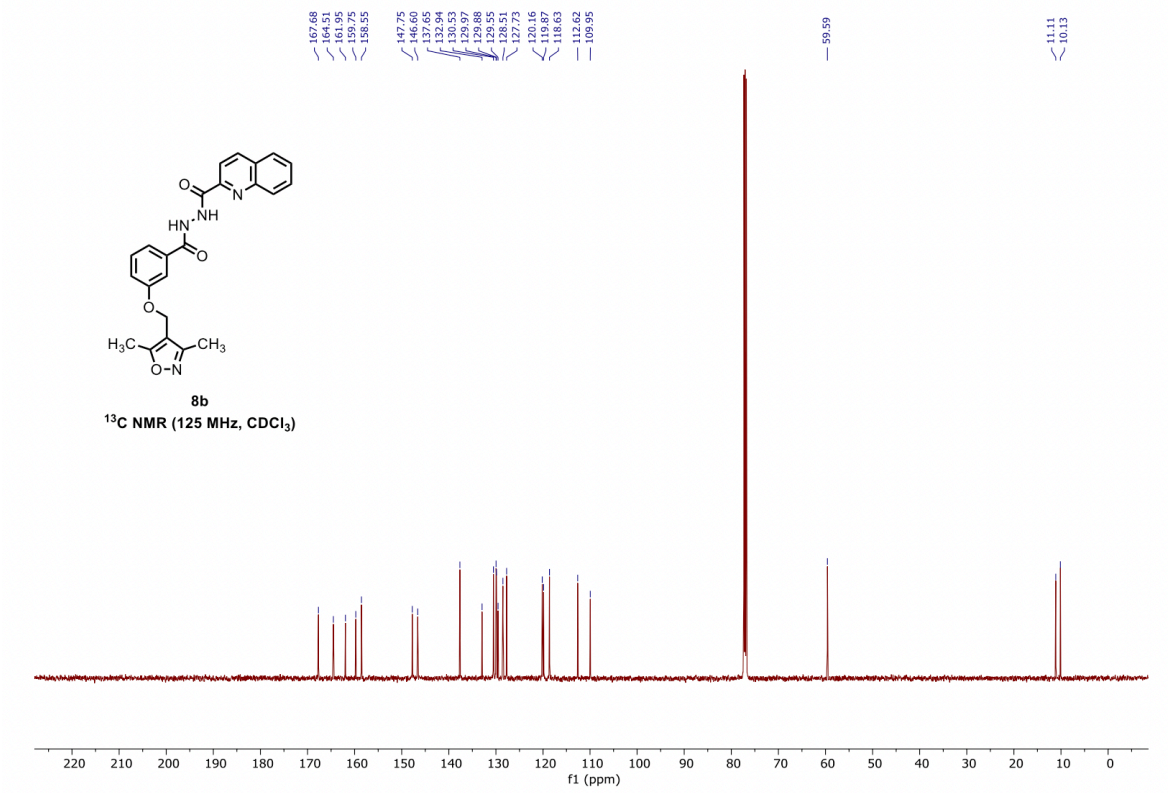

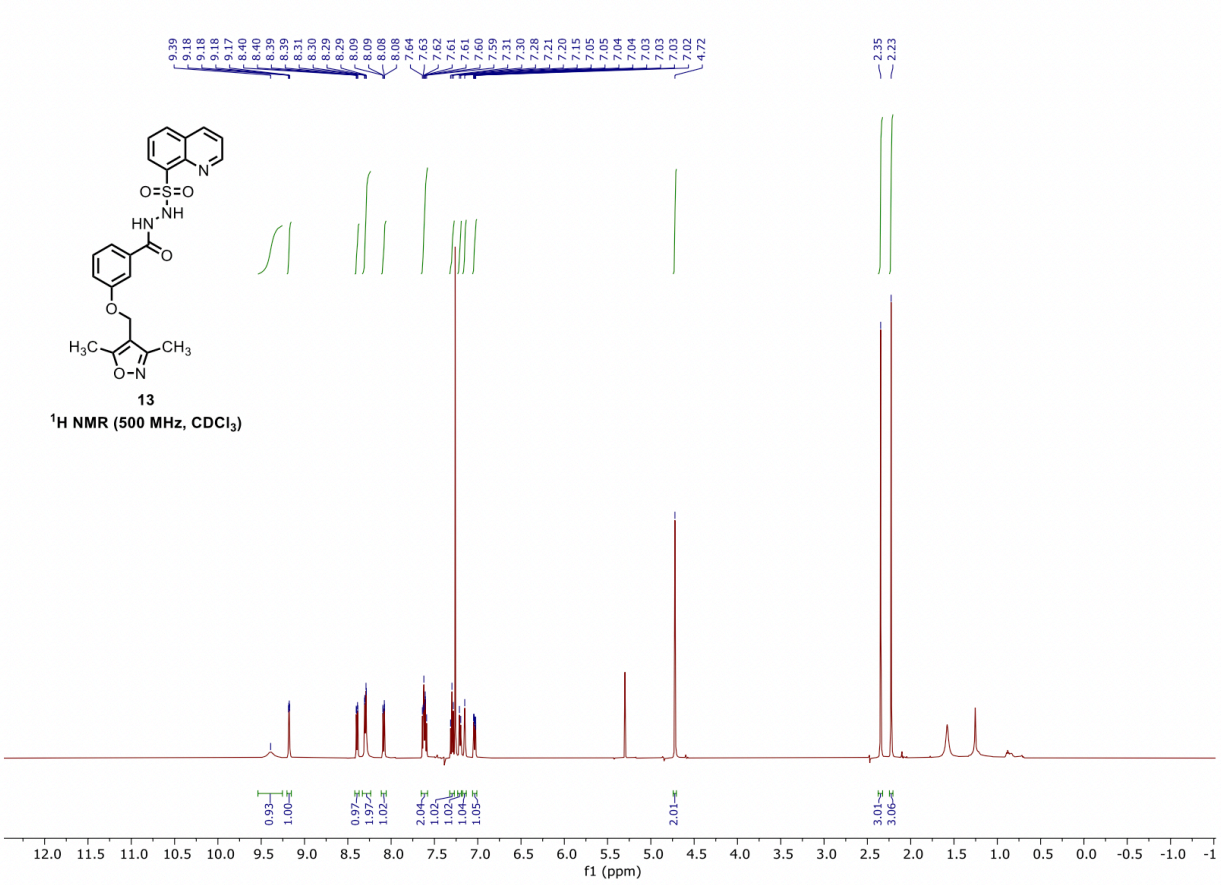
13
^{1}H NMR (500 MHz, CDCl$_3$)
f1 (ppm)

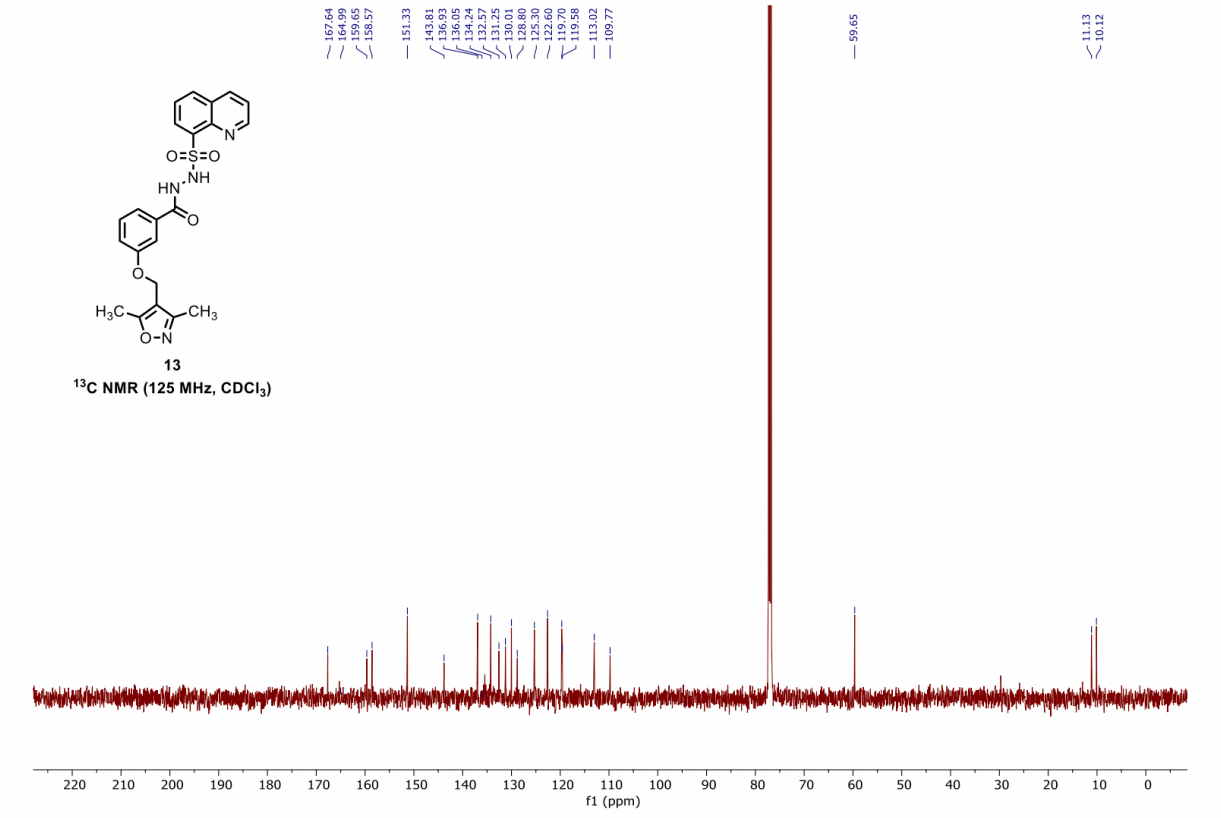
13
^{13}C NMR (125 MHz, CDCl$_3$)
f1 (ppm)

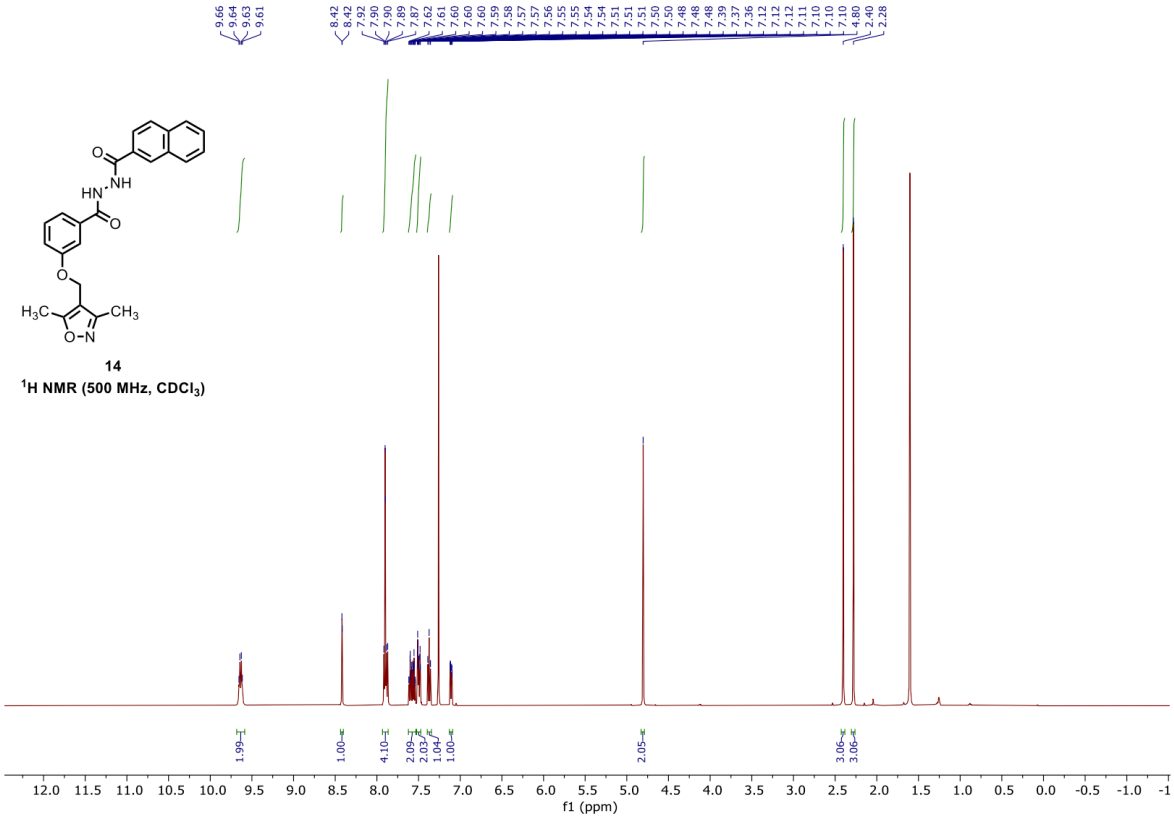
9.66
9.64
9.63
9.61
8.42
8.42
7.92
7.90
7.90
7.89
7.87
7.62
7.61
7.60
7.60
7.60
7.59
7.58
7.57
7.57
7.56
7.55
7.55
7.54
7.54
7.51
7.51
7.51
7.50
7.50
7.48
7.48
7.48
7.39
7.37
7.36
7.12
7.12
7.12
7.11
7.10
7.10
4.80
2.40
2.28
O
NH
HN
O
O
H3C
CH3
O-N
14
1H NMR (500 MHz, CDCl3)
1.99
1.00
4.10
2.09
2.03
1.04
1.00
2.05
3.06
3.06
12.0 11.5 11.0 10.5 10.0 9.5 9.0 8.5 8.0 7.5 7.0 6.5 6.0 5.5 5.0 4.5 4.0 3.5 3.0 2.5 2.0 1.5 1.0 0.5 0.0 -0.5 -1.0 -1
f1 (ppm)

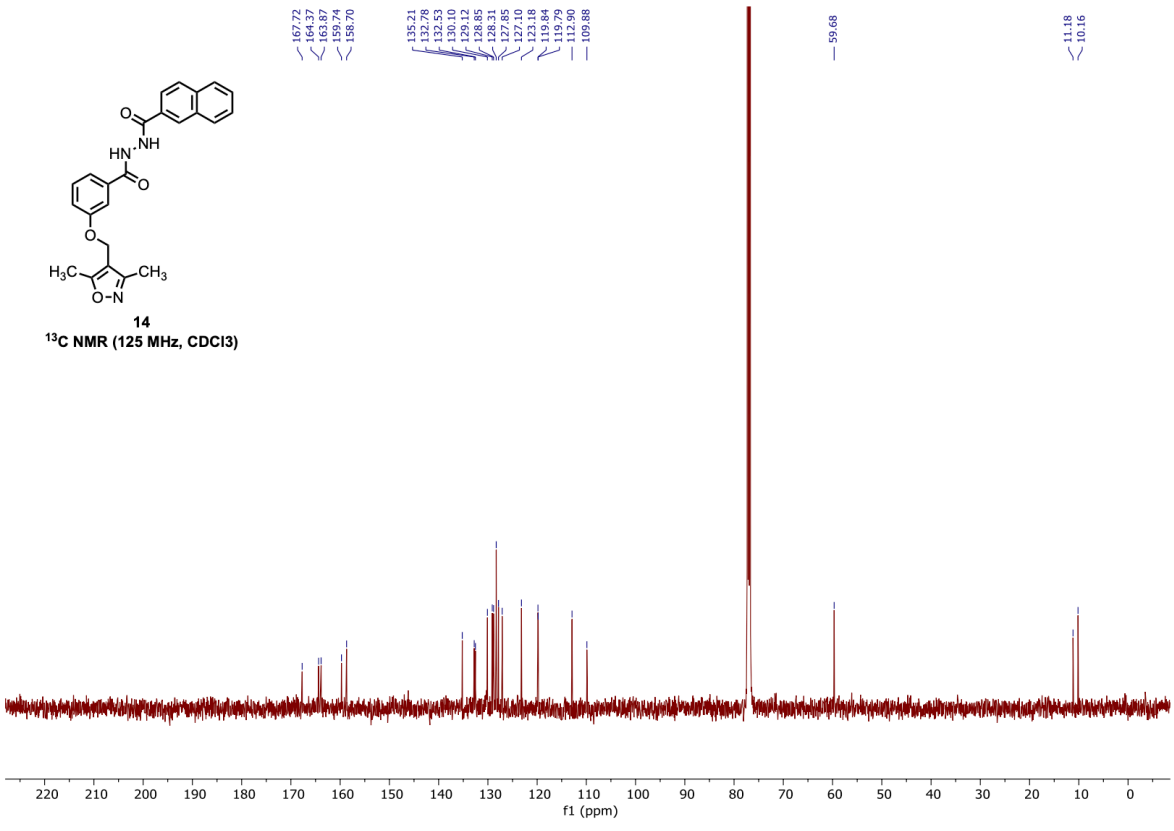
167.72
164.37
163.87
159.74
158.70
135.21
132.78
132.53
130.10
129.12
128.85
128.31
127.85
127.10
123.18
119.84
119.79
112.99
109.88
59.68
11.18
10.16
O
NH
HN
O
O
H3C
CH3
O-N
14
13C NMR (125 MHz, CDCl3)
220 210 200 190 180 170 160 150 140 130 120 110 100 90 80 70 60 50 40 30 20 10 0
f1 (ppm)

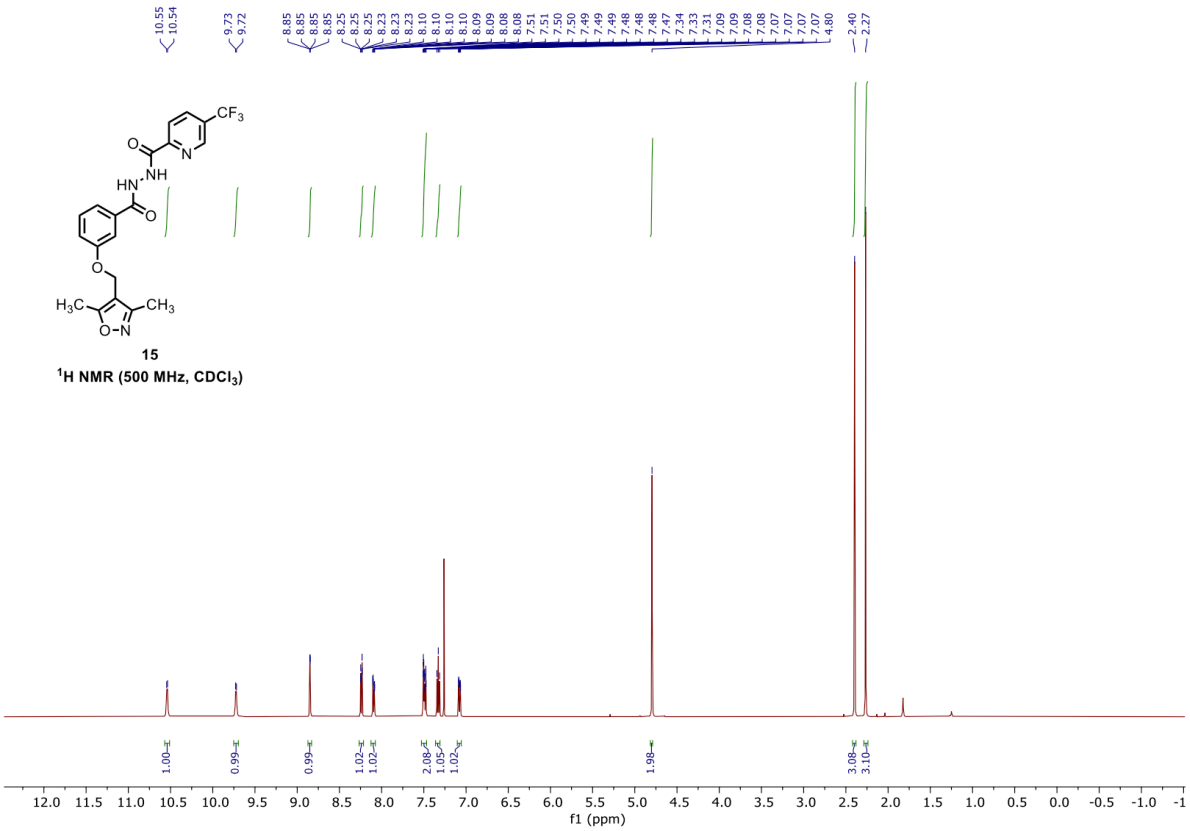

15

^{1}H NMR (500 MHz, $CDCl_3$)

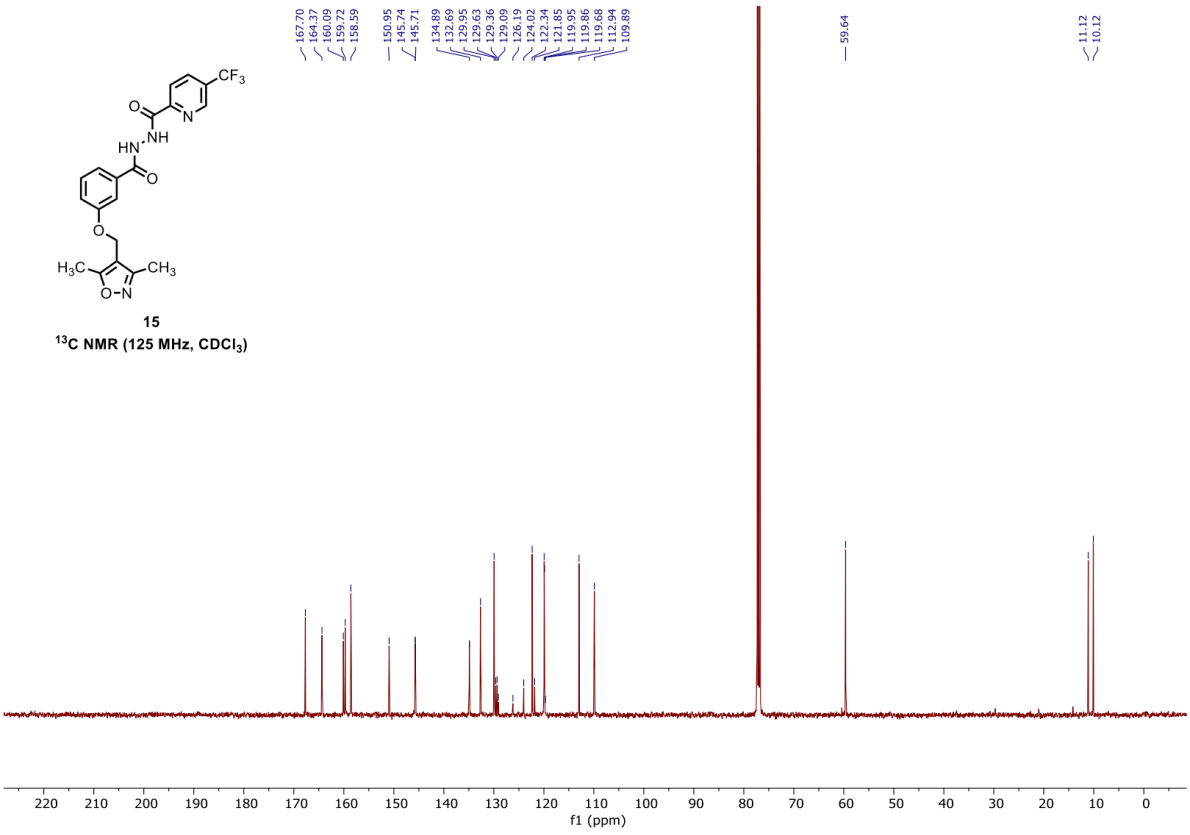

15

^{13}C NMR (125 MHz, $CDCl_3$)

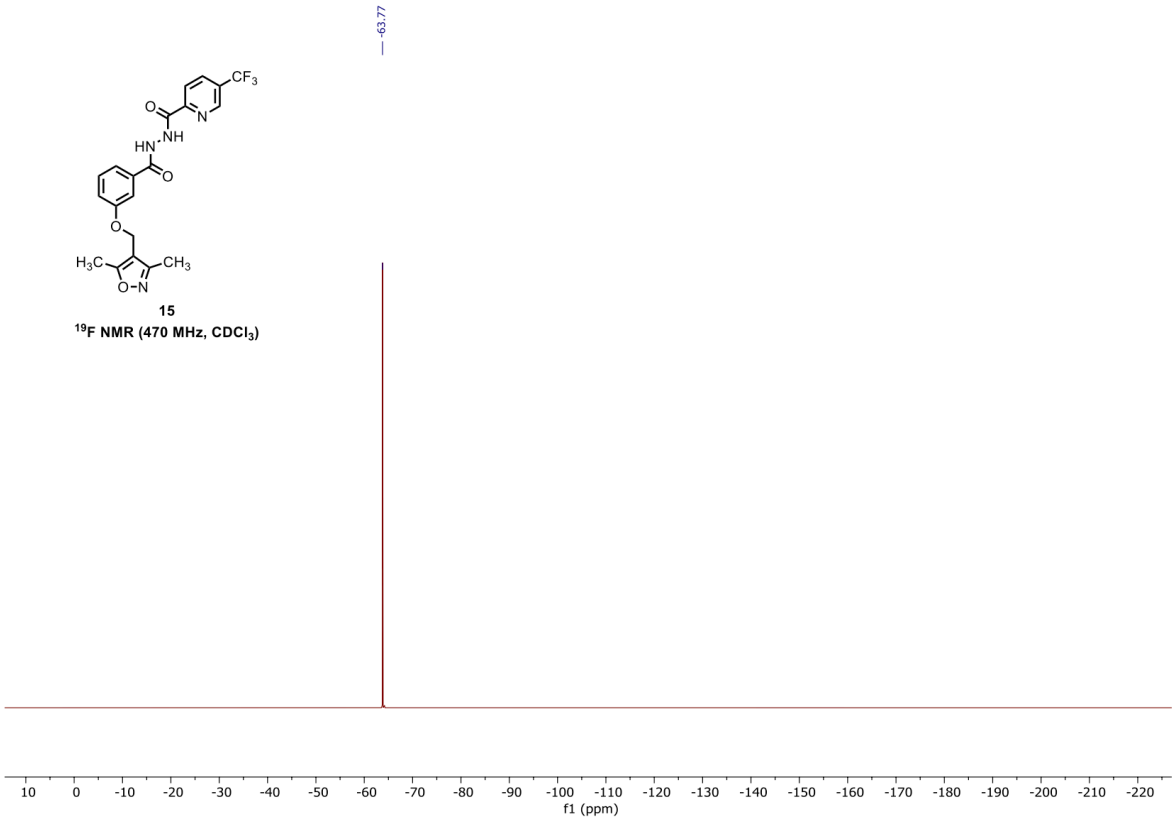

15

^{19}F NMR (470 MHz, $CDCl_3$)

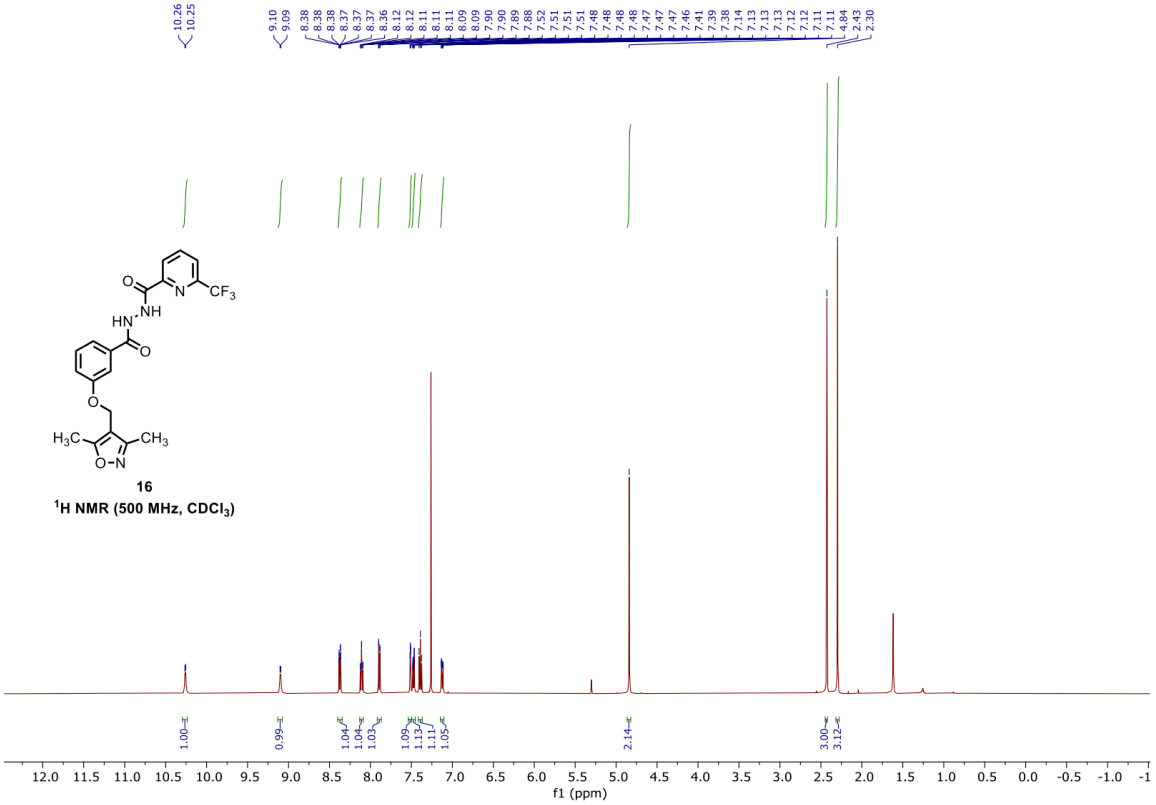
16
1H NMR (500 MHz, CDCl3)
f1 (ppm)

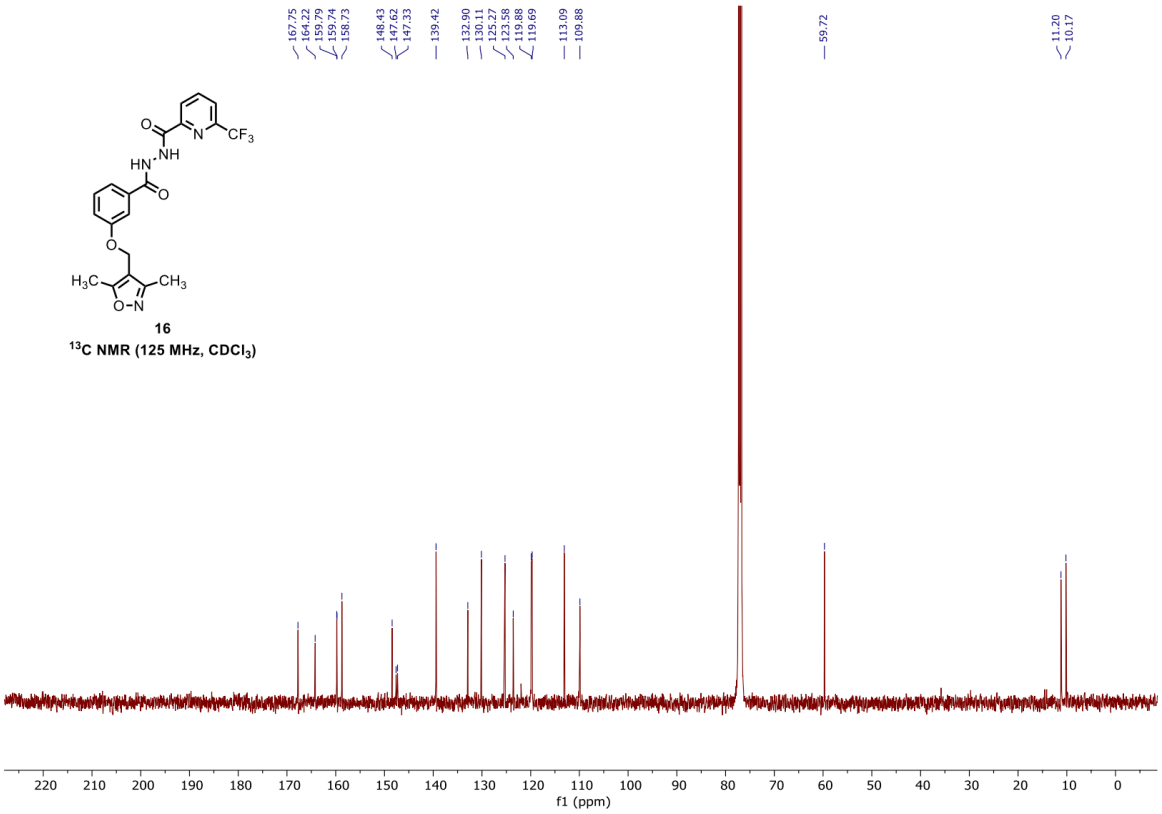
16
13C NMR (125 MHz, CDCl3)
f1 (ppm)

16

^{19}F NMR (470 MHz, $CDCl_3$)

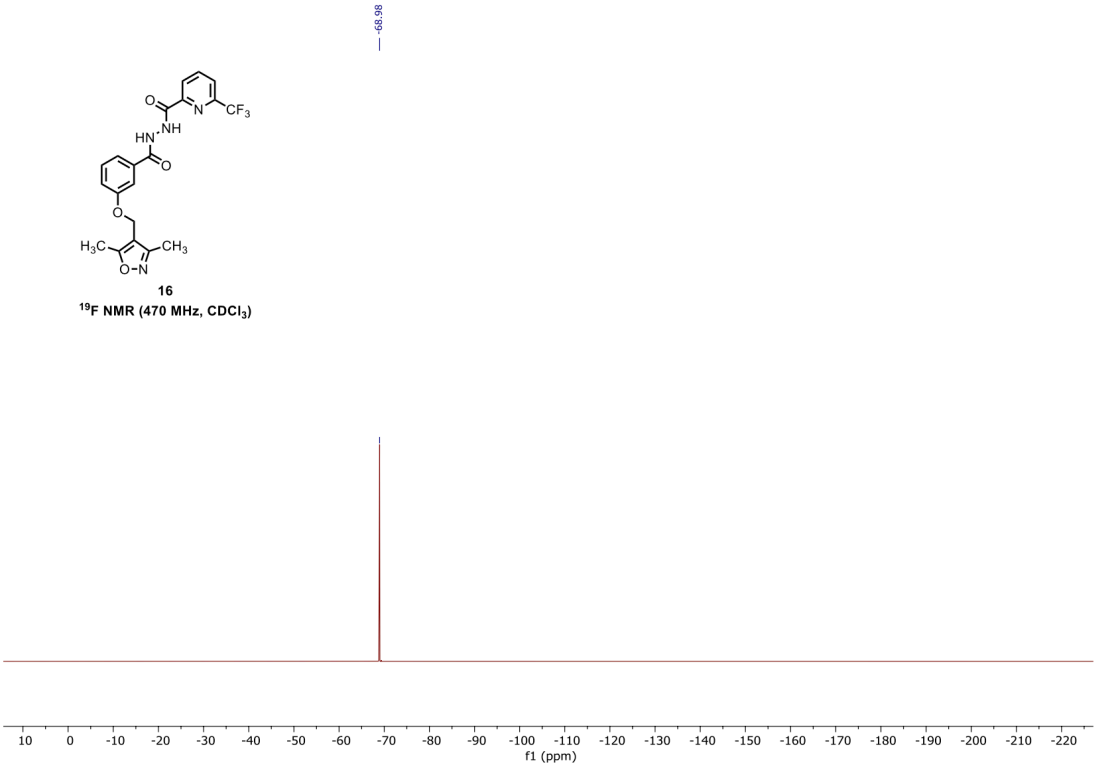

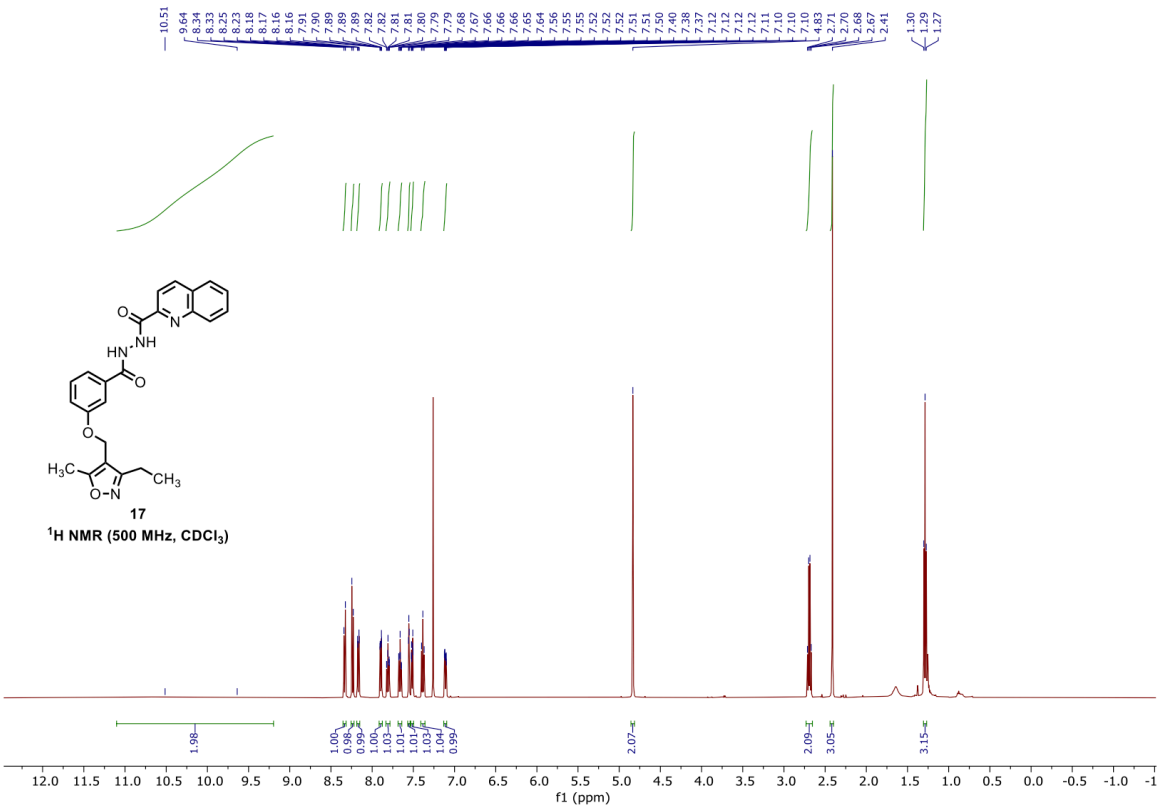
17
1H NMR (500 MHz, CDCl3)
f1 (ppm)

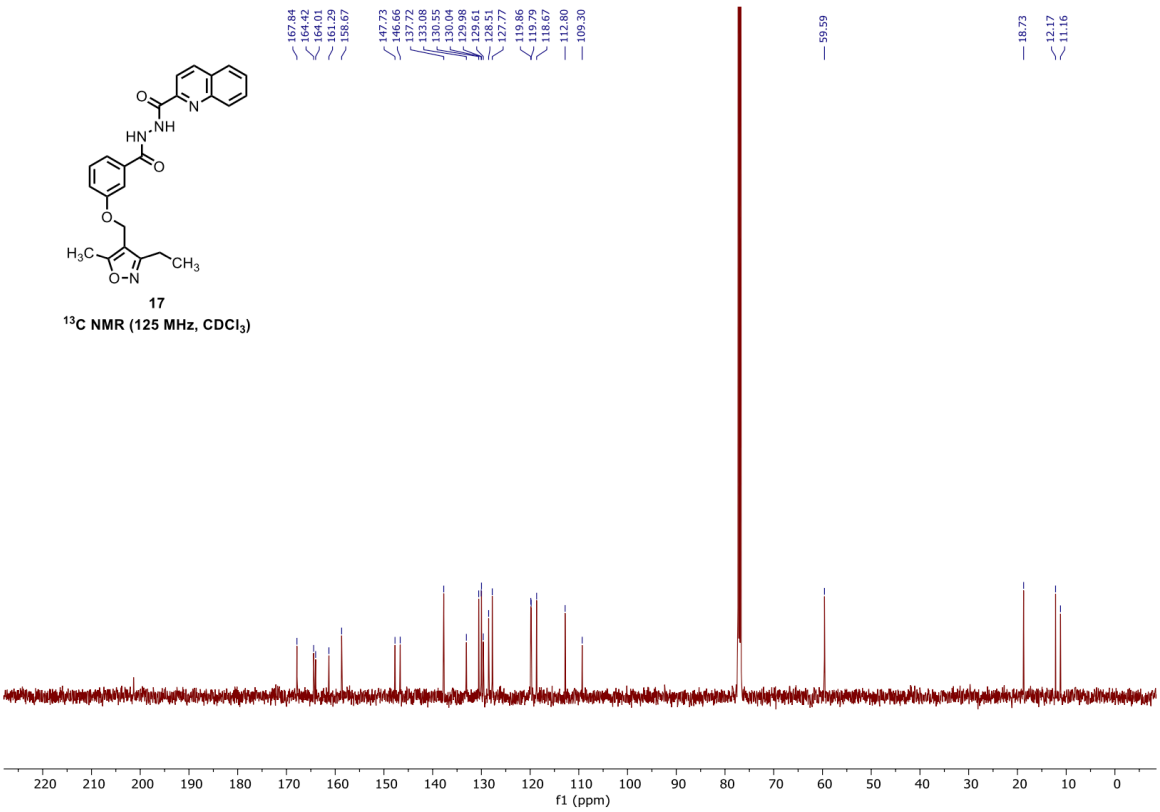
17
13C NMR (125 MHz, CDCl3)
f1 (ppm)

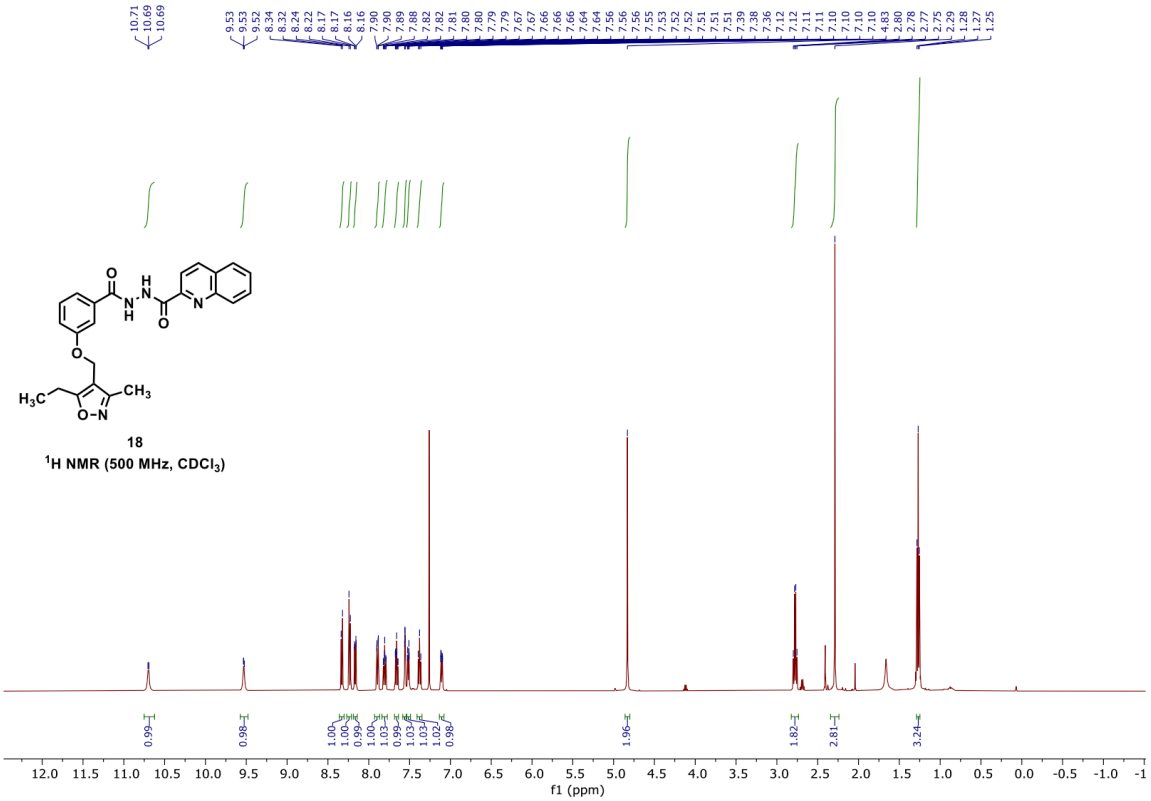
18
^{1}H NMR (500 MHz, CDCl$_3$)
f1 (ppm)

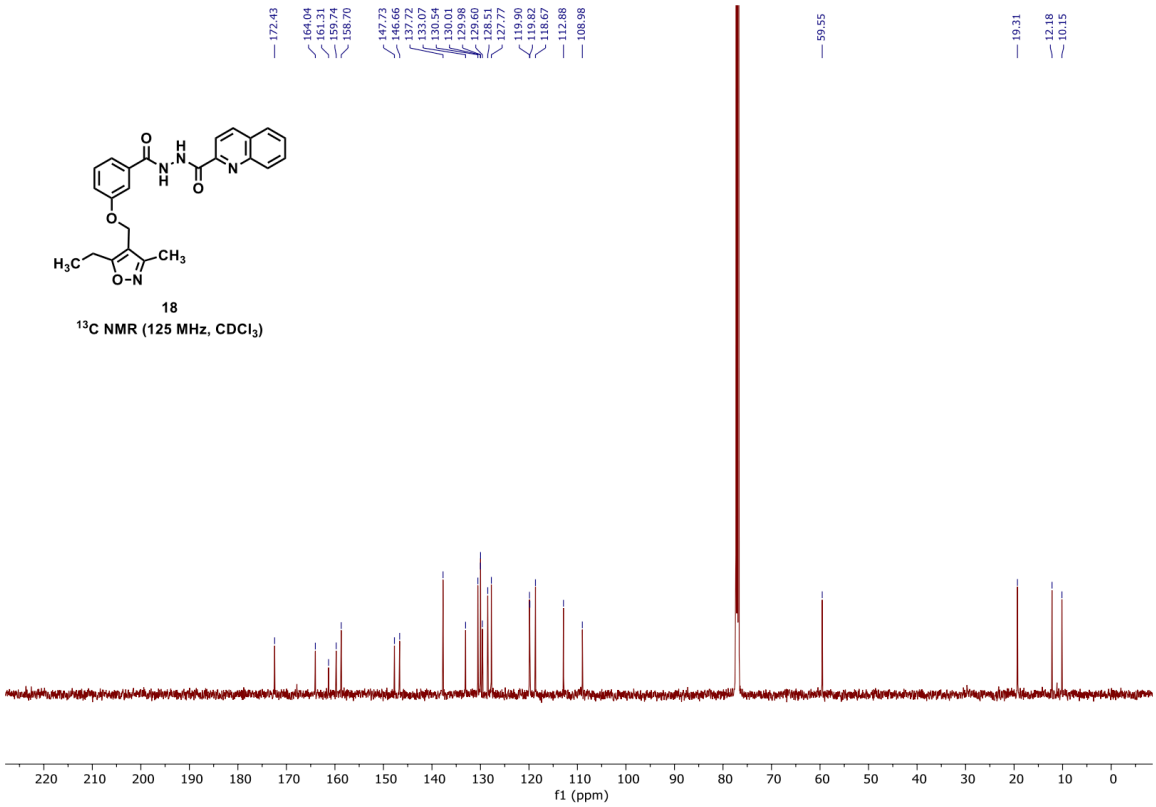
18
^{13}C NMR (125 MHz, CDCl$_3$)
f1 (ppm)

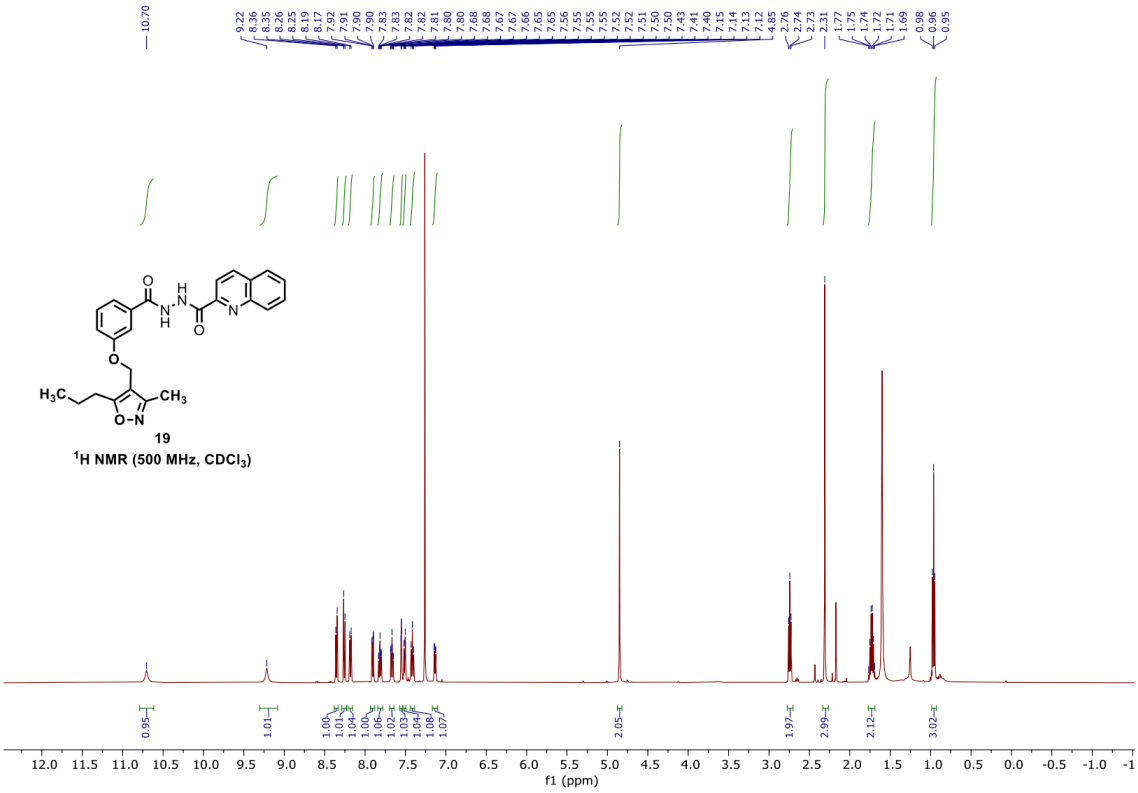

19

^{1}H NMR (500 MHz, $CDCl_3$)

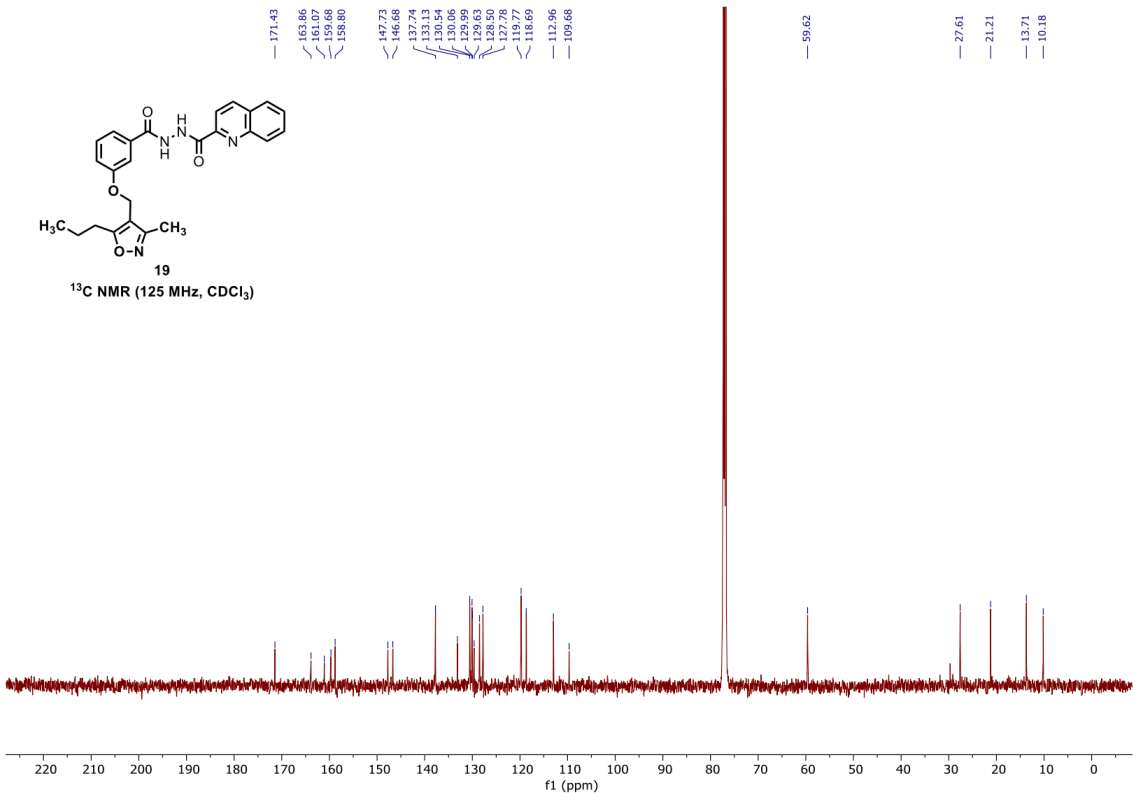

19

^{13}C NMR (125 MHz, $CDCl_3$)

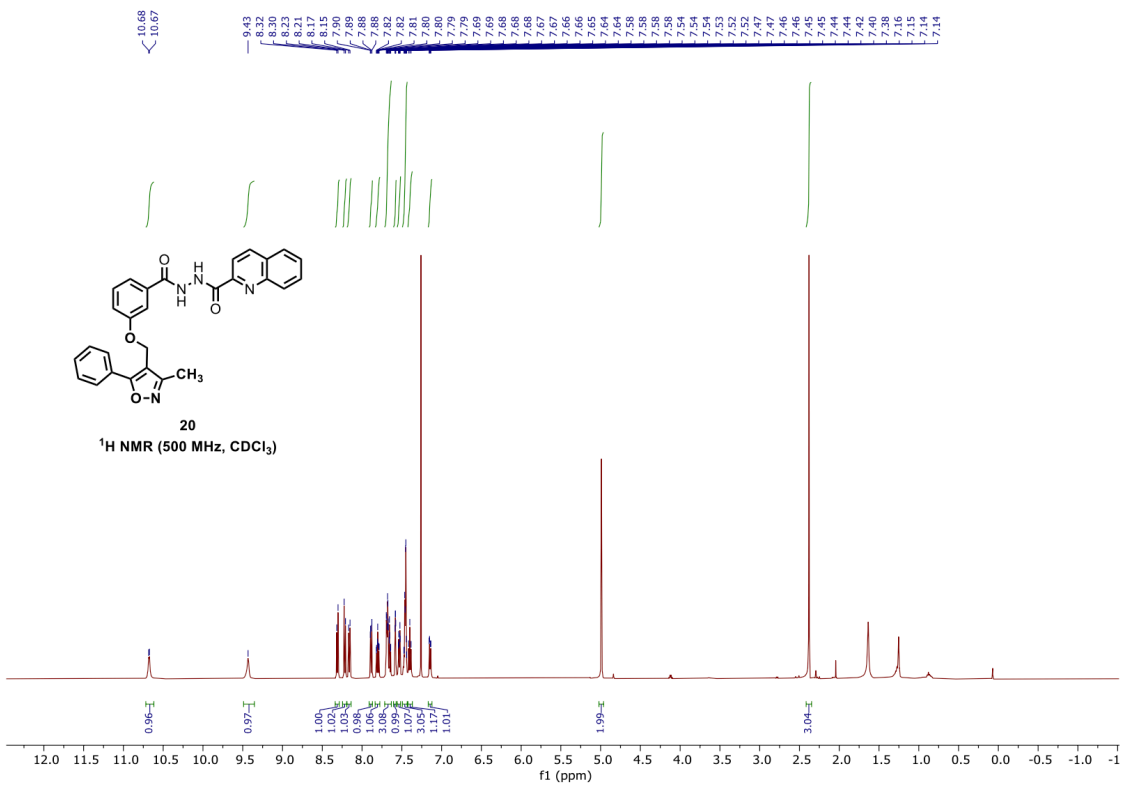

20

^{1}H NMR (500 MHz, $CDCl_3$)

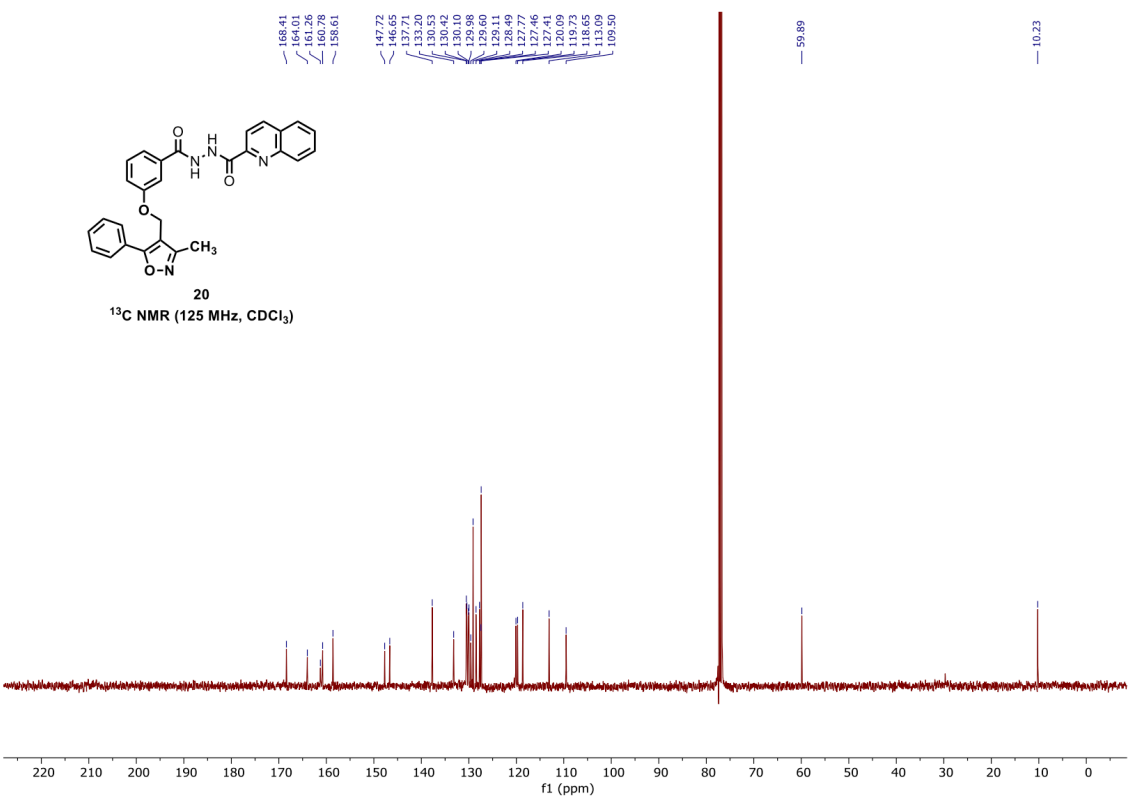

20

^{13}C NMR (125 MHz, $CDCl_3$)

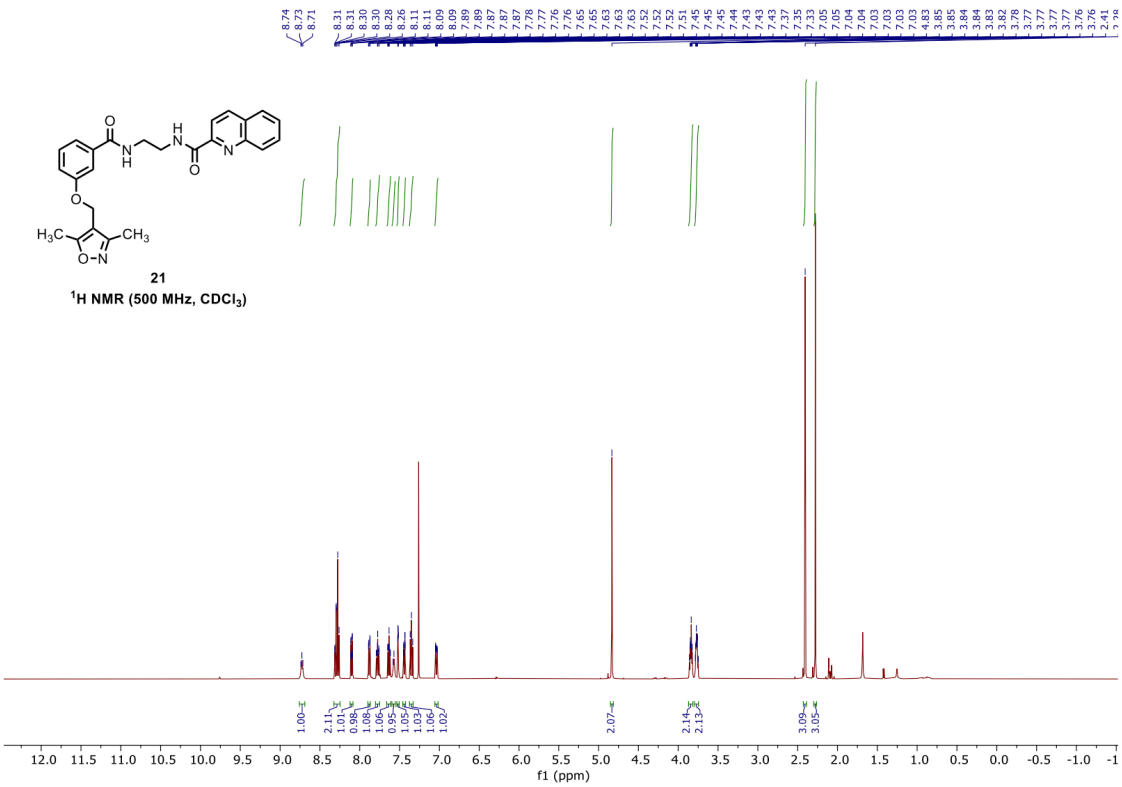
21
1H NMR (500 MHz, CDCl3)
f1 (ppm)

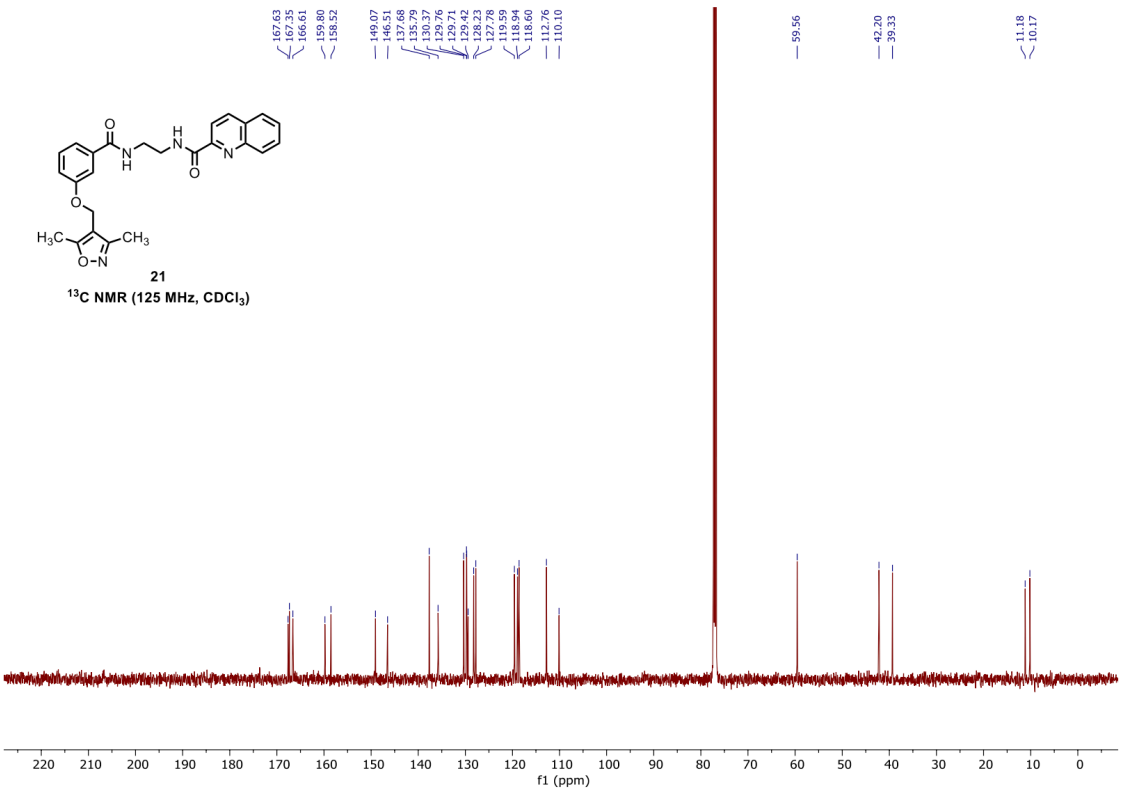
21
13C NMR (125 MHz, CDCl3)
f1 (ppm)

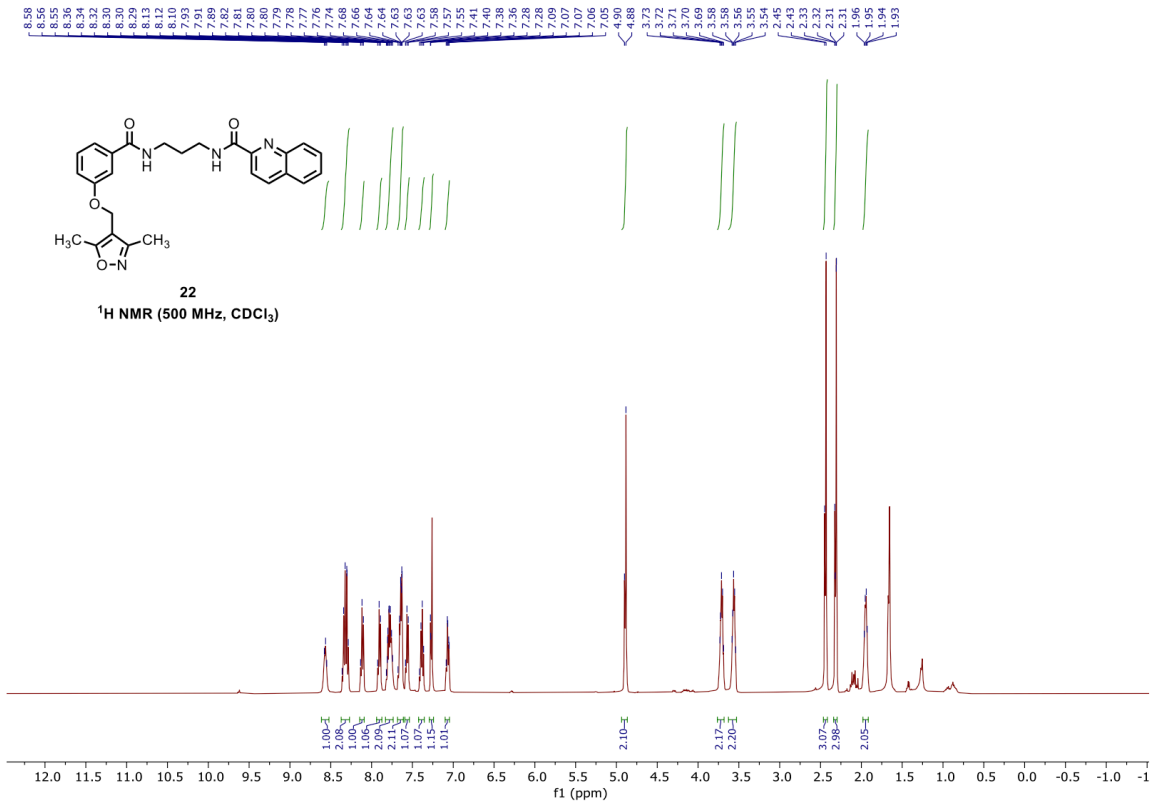

22

^{1}H NMR (500 MHz, $CDCl_3$)

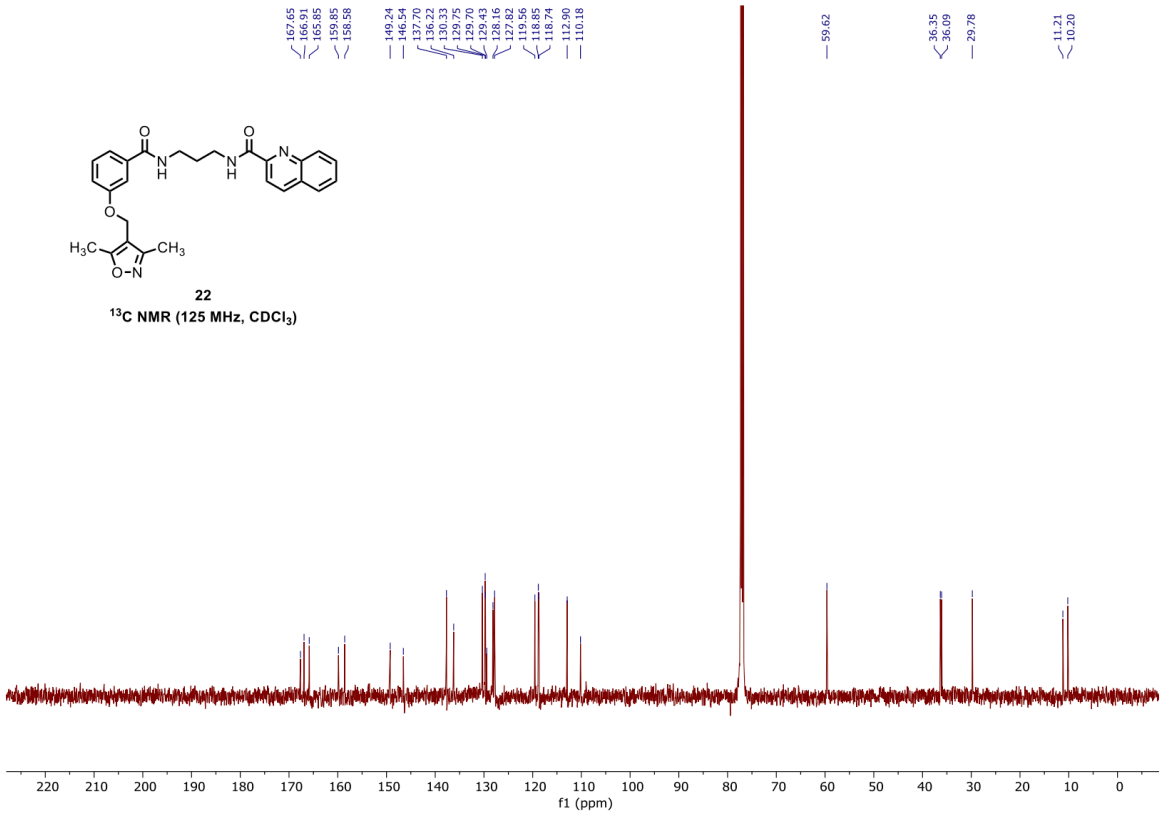

22

^{13}C NMR (125 MHz, $CDCl_3$)

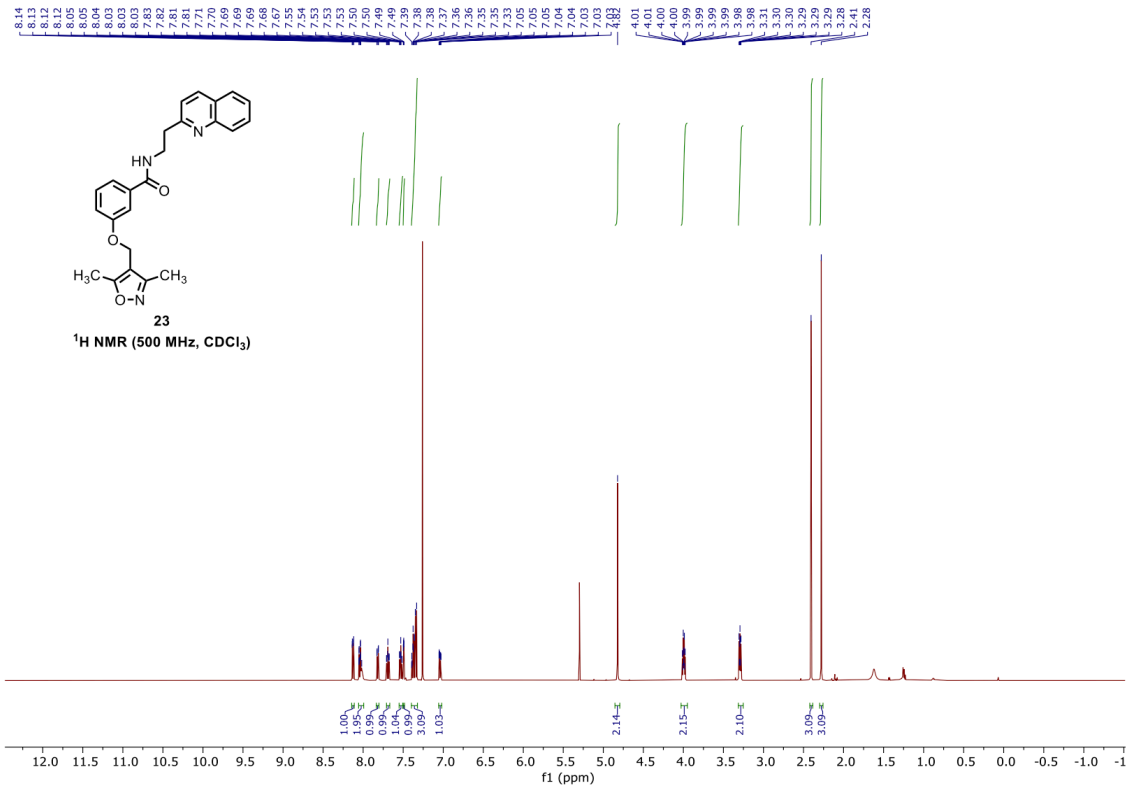
23
^{1}H NMR (500 MHz, CDCl$_3$)
f1 (ppm)

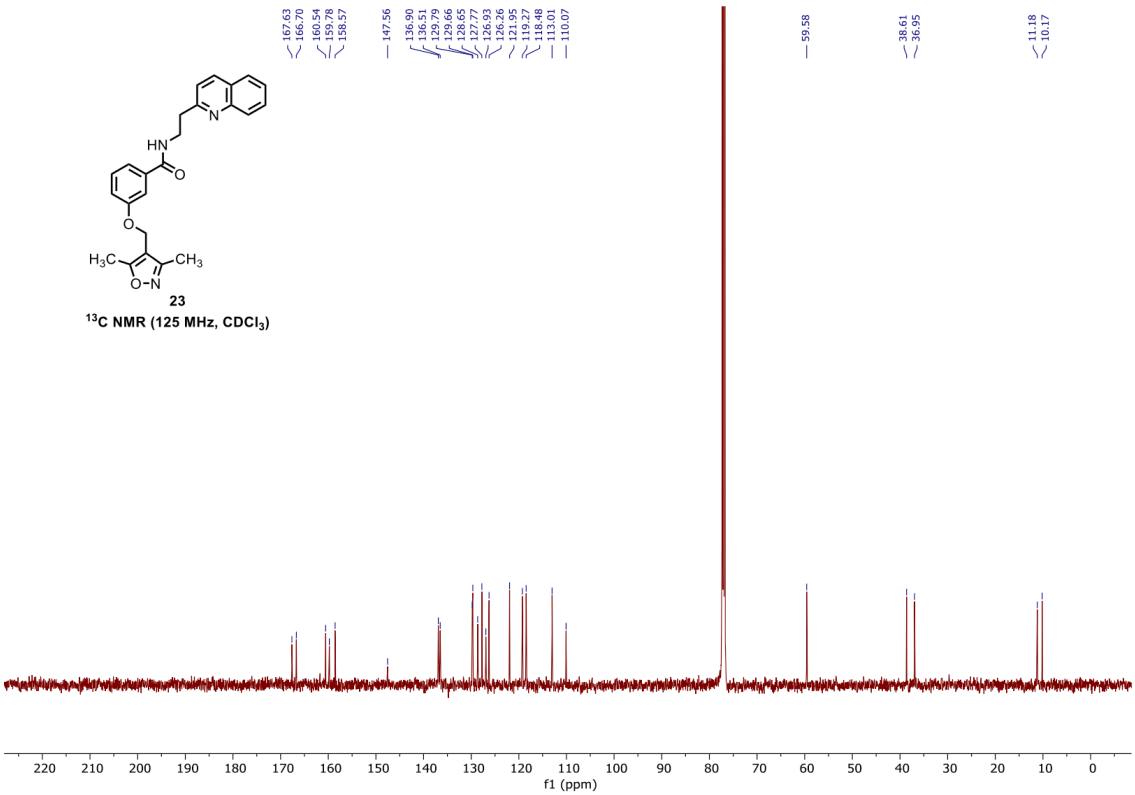
23
^{13}C NMR (125 MHz, CDCl$_3$)
f1 (ppm)

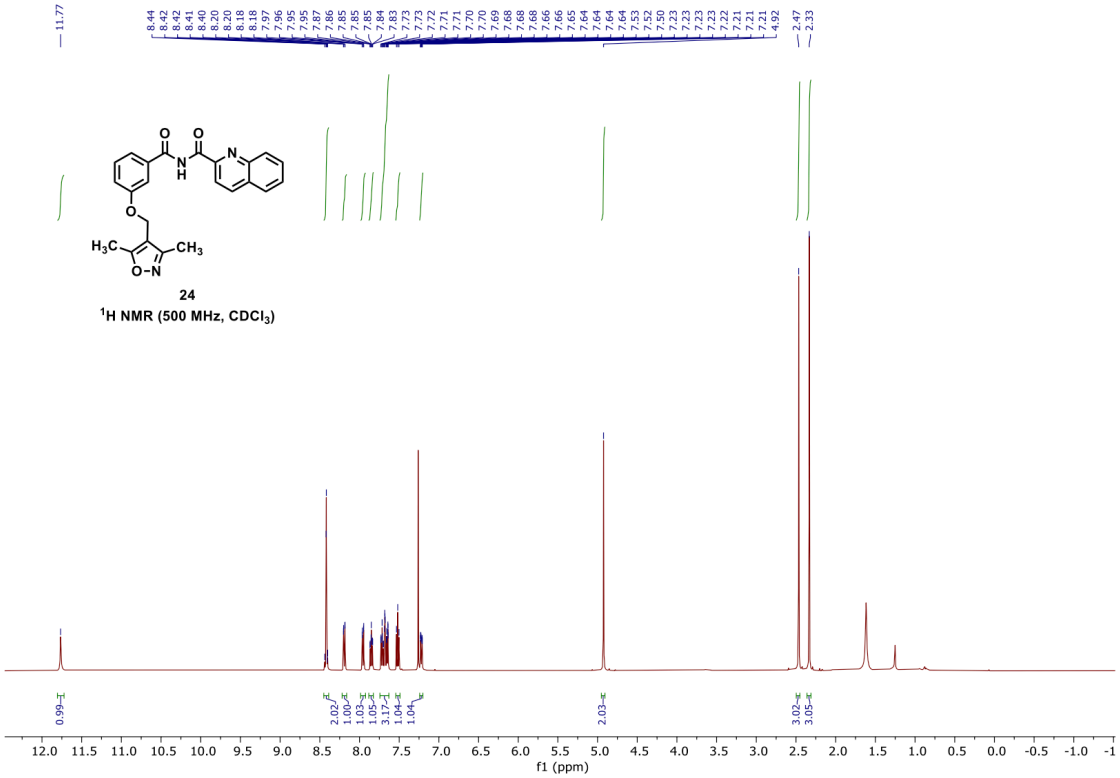
11.77
8.44 8.42 8.42 8.41 8.40 8.20 8.20 8.18 8.18 7.97 7.96 7.95 7.95 7.87 7.86 7.85 7.85 7.85 7.84 7.83 7.73 7.73 7.72 7.71 7.71 7.70 7.70 7.69 7.68 7.68 7.68 7.66 7.66 7.65 7.64 7.64 7.64 7.53 7.52 7.50 7.23 7.23 7.23 7.22 7.21 7.21 7.21 4.92
2.47
2.33
O
O
N
H
N
O
H3C
CH3
O–N
24
1H NMR (500 MHz, CDCl3)
0.99
2.02
1.00
1.03
1.05
3.17
1.04
1.04
2.03
3.02
3.05
12.0 11.5 11.0 10.5 10.0 9.5 9.0 8.5 8.0 7.5 7.0 6.5 6.0 5.5 5.0 4.5 4.0 3.5 3.0 2.5 2.0 1.5 1.0 0.5 0.0 -0.5 -1.0 -1
f1 (ppm)

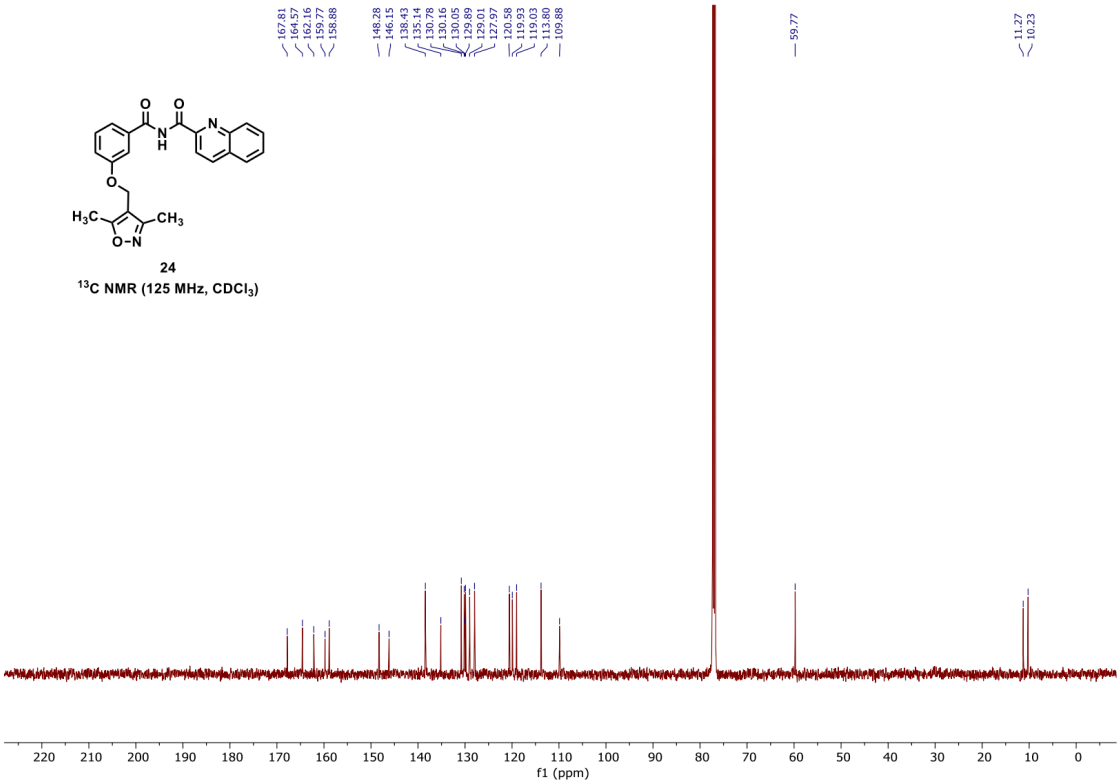
167.81
164.57
162.16
159.77
158.88
148.28
146.15
138.43
135.14
130.78
130.16
130.05
129.89
129.01
127.97
120.58
119.93
119.03
113.80
109.88
59.77
11.27
10.23
O
O
N
H
N
O
H3C
CH3
O–N
24
13C NMR (125 MHz, CDCl3)
220 210 200 190 180 170 160 150 140 130 120 110 100 90 80 70 60 50 40 30 20 10 0
f1 (ppm)

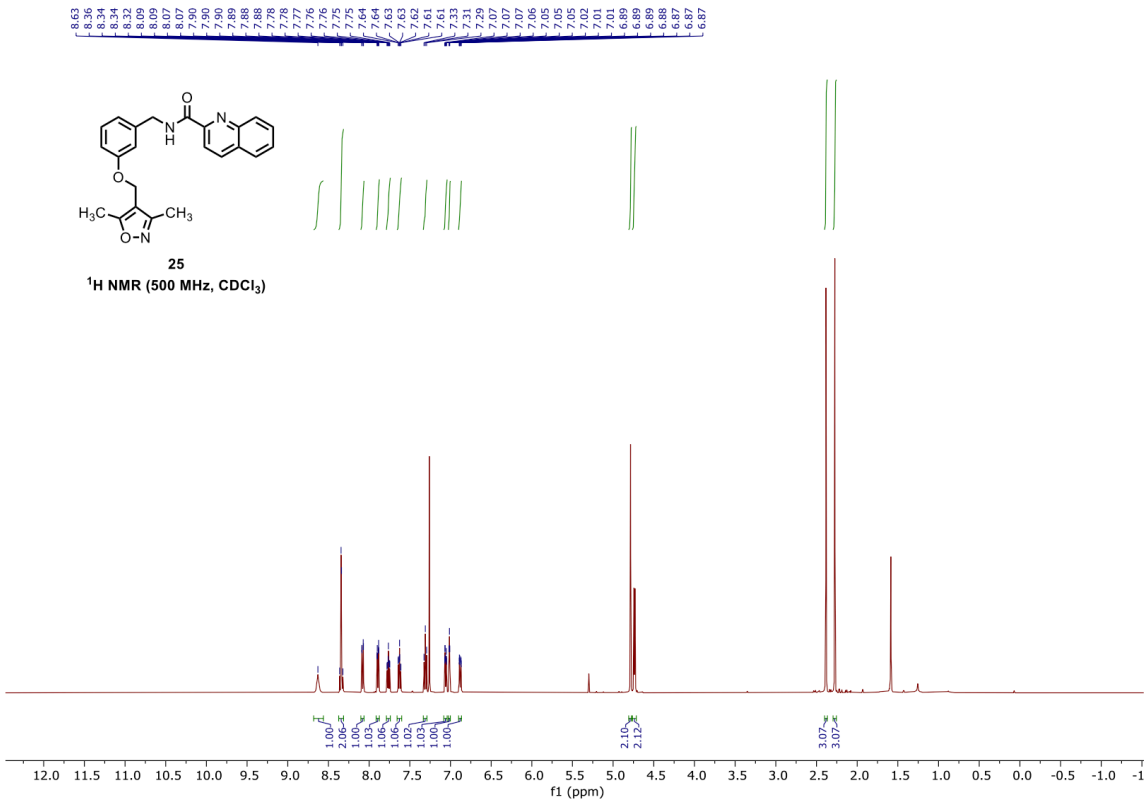
8.63 8.36 8.34 8.34 8.32 8.09 8.09 8.07 8.07 7.90 7.90 7.90 7.89 7.88 7.88 7.78 7.78 7.77 7.77 7.76 7.76 7.75 7.75 7.64 7.64 7.63 7.63 7.62 7.61 7.61 7.33 7.31 7.29 7.07 7.07 7.07 7.06 7.05 7.05 7.05 7.02 7.01 7.01 6.89 6.89 6.89 6.88 6.87 6.87 6.87
25
^{1}H NMR (500 MHz, CDCl$_3$)
1.00 2.06 1.00 1.03 1.06 1.06 1.03 1.00 1.00
2.10 2.12
3.07 3.07
f1 (ppm)

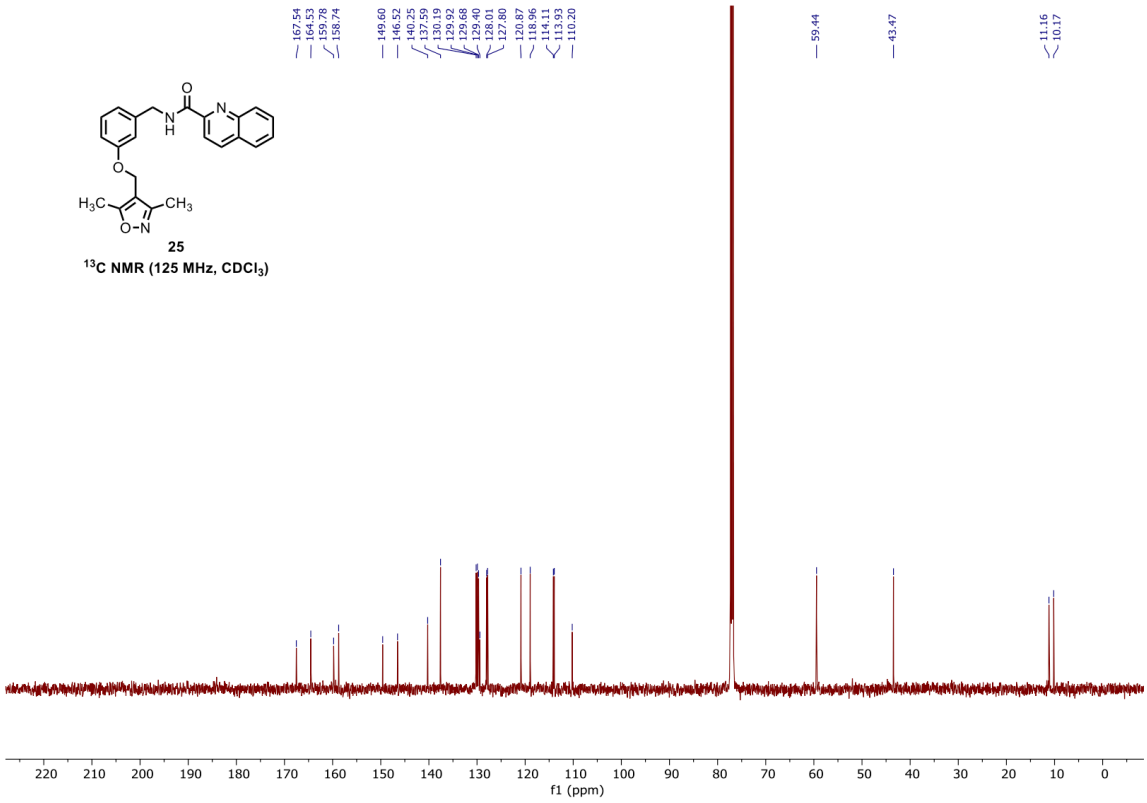
167.54 164.53 159.28 158.74 149.60 146.52 140.25 137.59 130.19 129.82 129.68 129.40 128.01 127.80 120.87 118.96 114.11 113.93 110.20 59.44 43.47 11.16 10.17
25
^{13}C NMR (125 MHz, CDCl$_3$)
f1 (ppm)

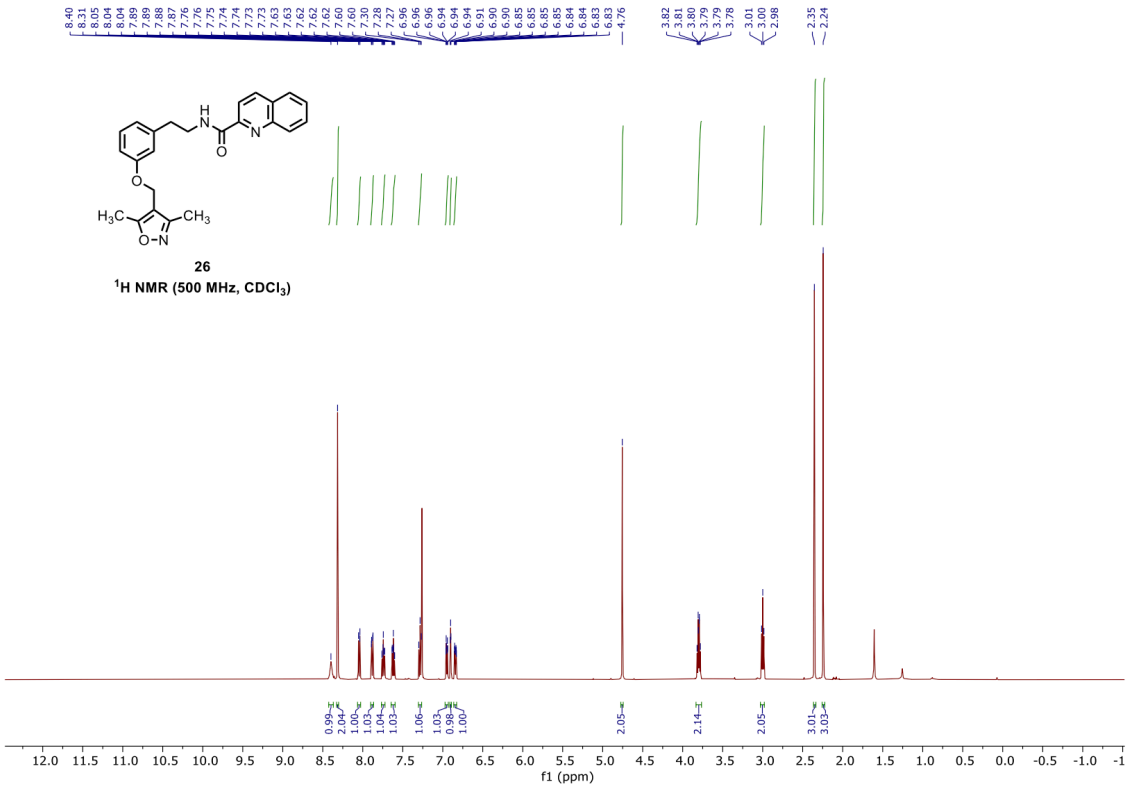

26

^{1}H NMR (500 MHz, $CDCl_3$)

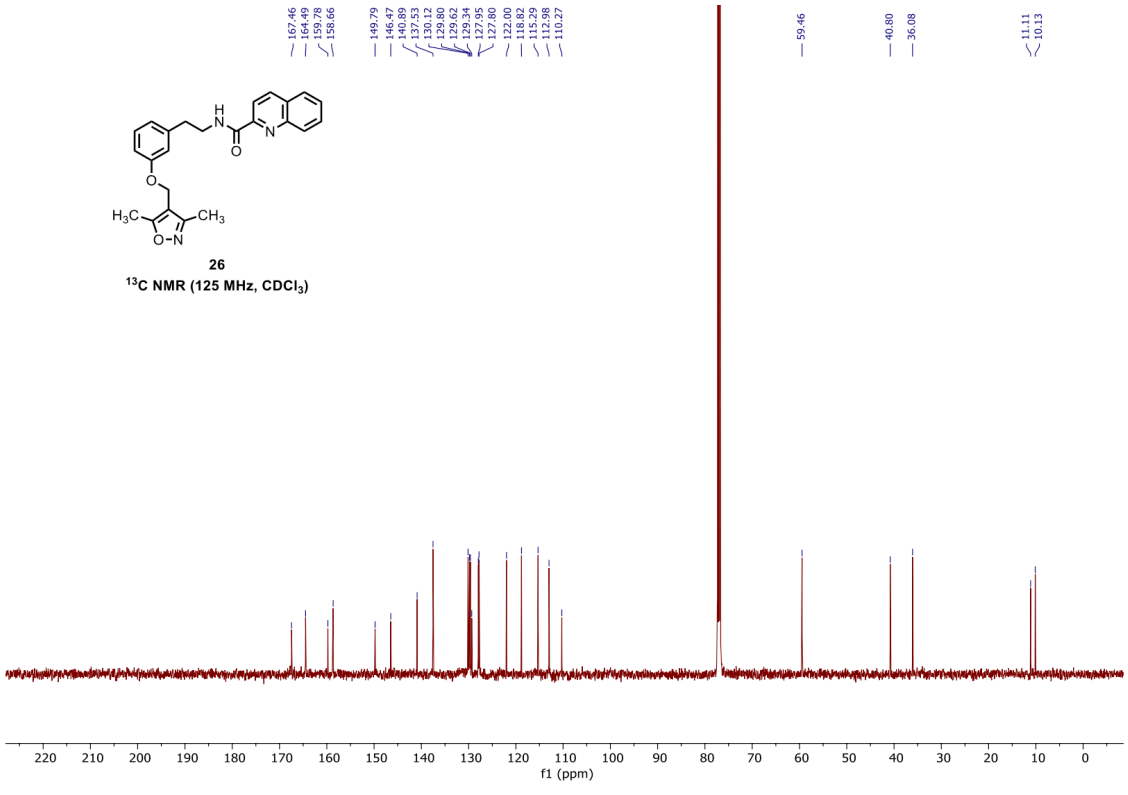

26

^{13}C NMR (125 MHz, $CDCl_3$)

HPLC Traces

Compound 08 was analyzed using a ThermoScientific Hypersil GOLDC18 column and a gradient of 95:5 to 5:95 H_2O:ACN.

All other compounds were analyzed using a ZORBAX RRHT Eclipse XDB-C_{18} column and a gradient of 95:5 to 5:95 H_2O:MeCN

8 / 8b

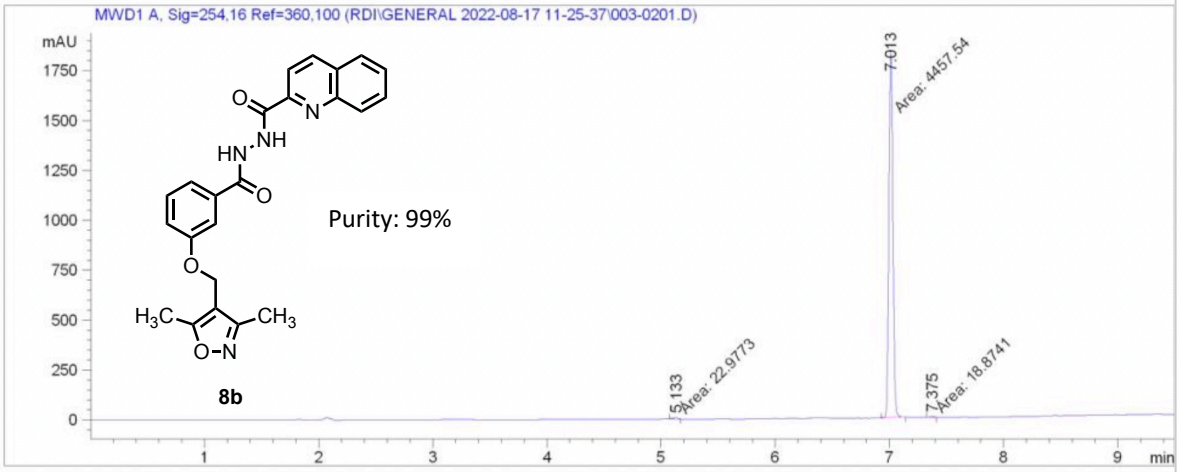


```
=====================================================================
                    Area Percent Report
=====================================================================

Sorted By             :      Signal
Multiplier:                   :      1.0000
Dilution:                     :      1.0000
Use Multiplier & Dilution Factor with ISTDs


Signal 1: MWD1 A, Sig=254,16 Ref=360,100

Peak RetTime Type  Width     Area      Height     Area
  #   [min]        [min]   [mAU*s]     [mAU]       %
----|-------|----|-------|----------|----------|--------|
   1   5.133 MM    0.0482   22.97734    7.95079   0.5107
   2   7.013 MM    0.0404 4457.53955 1839.15613  99.0698
   3   7.375 MM    0.0546   18.87412    5.76048   0.4195

Totals :                  4499.39102 1852.86740

=====================================================================
                        *** End of Report ***
```

13

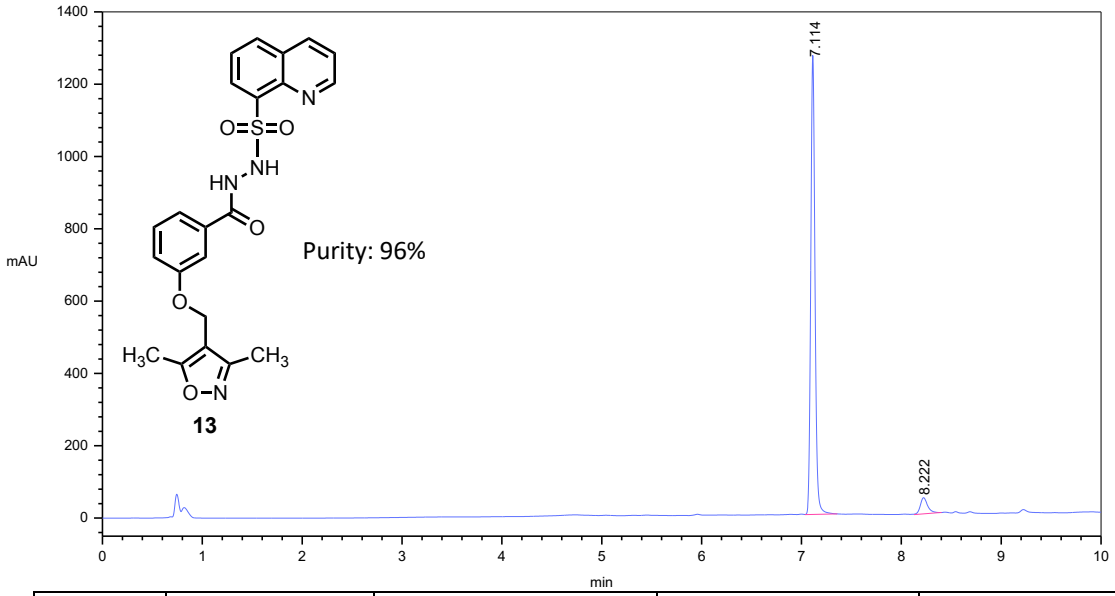

Peak	RetTime (min)	Area (mAU*s)	Height (mAU)	Area (%)
1	7.114	3705.53052	1271.52686	96.4761
2	8.222	135.34927	35.57998	3.5239

14

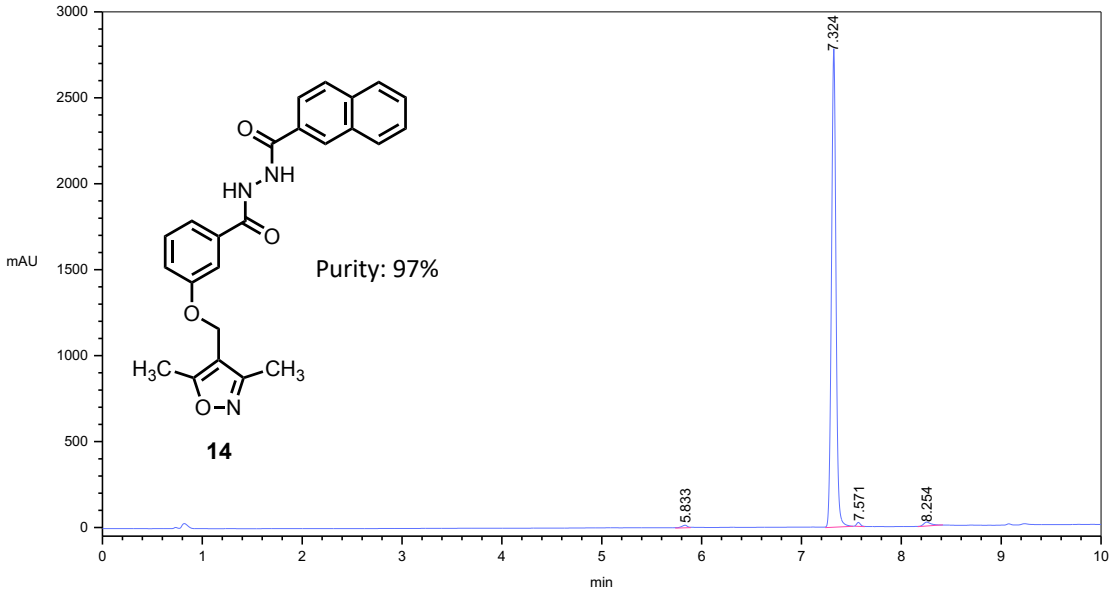

Peak	RetTime (min)	Area (mAU*s)	Height (mAU)	Area (%)
1	5.833	61.08140	15.20389	0.6894
2	7.324	8590.08398	2775.23120	96.9537
3	7.571	56.51580	21.47472	0.6379
4	8.254	152.30571	27.02657	1.7190

15

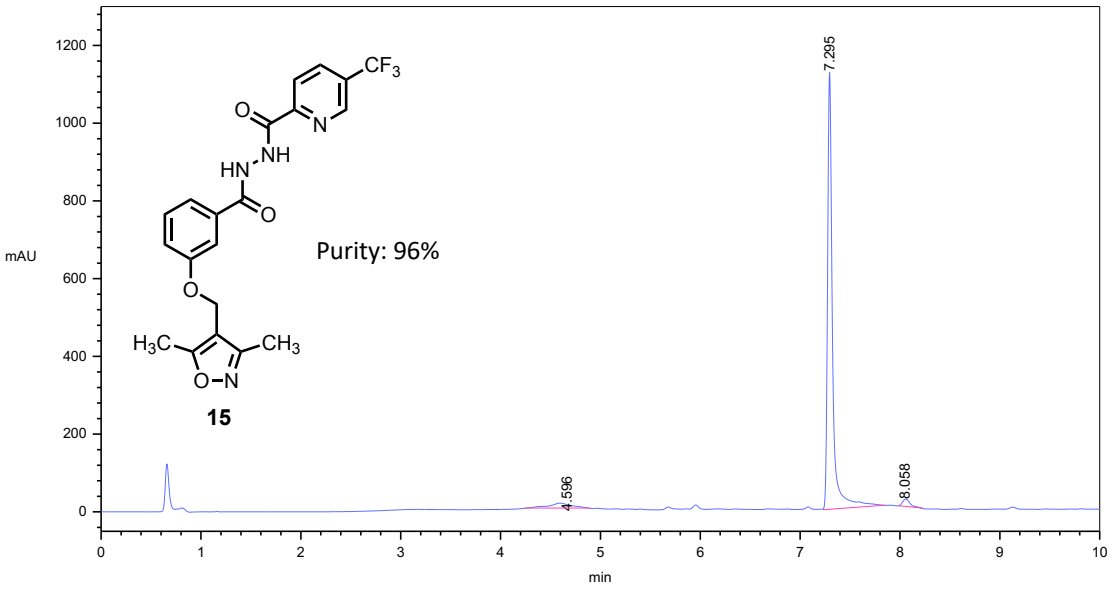

Peak	RetTime (min)	Area (mAU*s)	Height (mAU)	Area (%)
1	4.596	62.20026	7.93594	1.6179
2	7.295	3699.60425	1124.70386	96.2280
3	8.058	75.41700	17.86606	1.9616

16

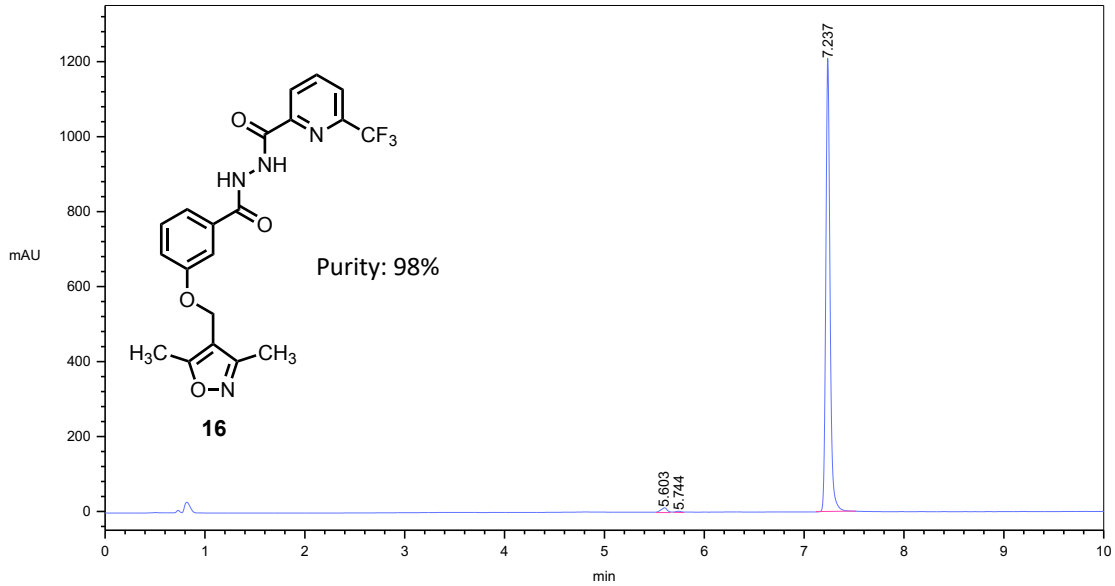

Peak	RetTime (min)	Area (mAU*s)	Height (mAU)	Area (%)
1	5.603	56.94898	12.59515	1.5413
2	5.744	32.49028	6.30248	0.8793
3	7.237	3605.36768	1210.73450	97.5793

17

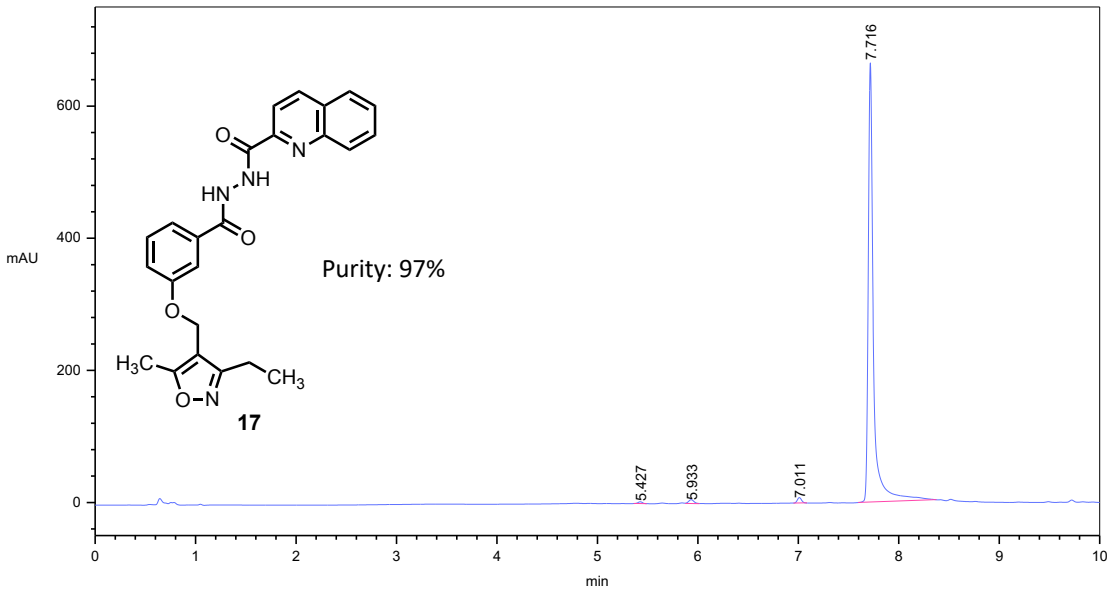

Peak	RetTime (min)	Area (mAU*s)	Height (mAU)	Area (%)
1	5.427	11.49231	3.64736	0.4777
2	5.933	31.63272	7.60844	1.3149
3	7.011	24.67721	8.18935	1.0258
4	7.716	2337.91943	665.76617	97.1816

18

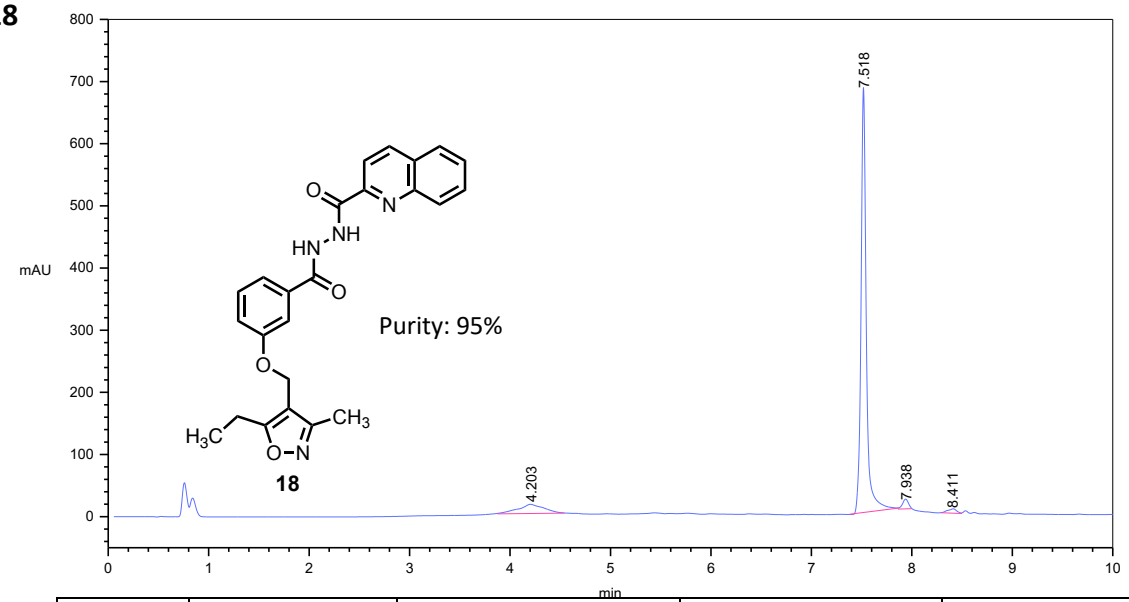

Peak	RetTime (min)	Area (mAU*s)	Height (mAU)	Area (%)
1	4.203	85.08701	8.64702	3.2319
2	7.518	2501.45166	684.45831	95.0142
3	7.938	26.94125	9.78608	1.0233
4	8.411	19.23445	4.65337	0.7306

19

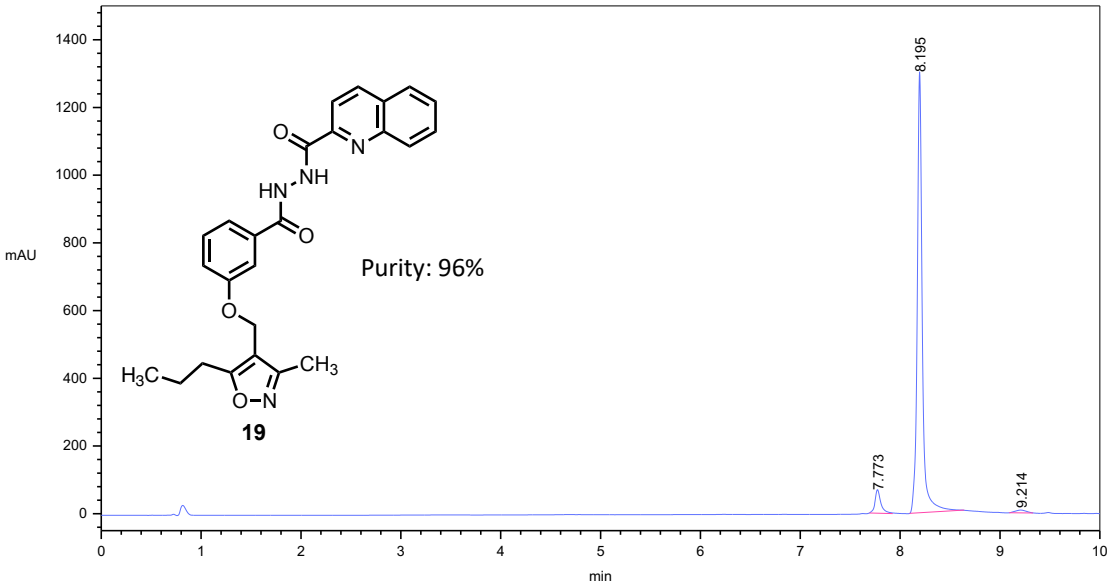

Peak	RetTime (min)	Area (mAU*s)	Height (mAU)	Area (%)
1	7.773	163.93793	56.67533	3.4324
2	8.195	4564.75448	1304.48206	95.5730
3	9.214	47.50674	7.12561	0.9947

20

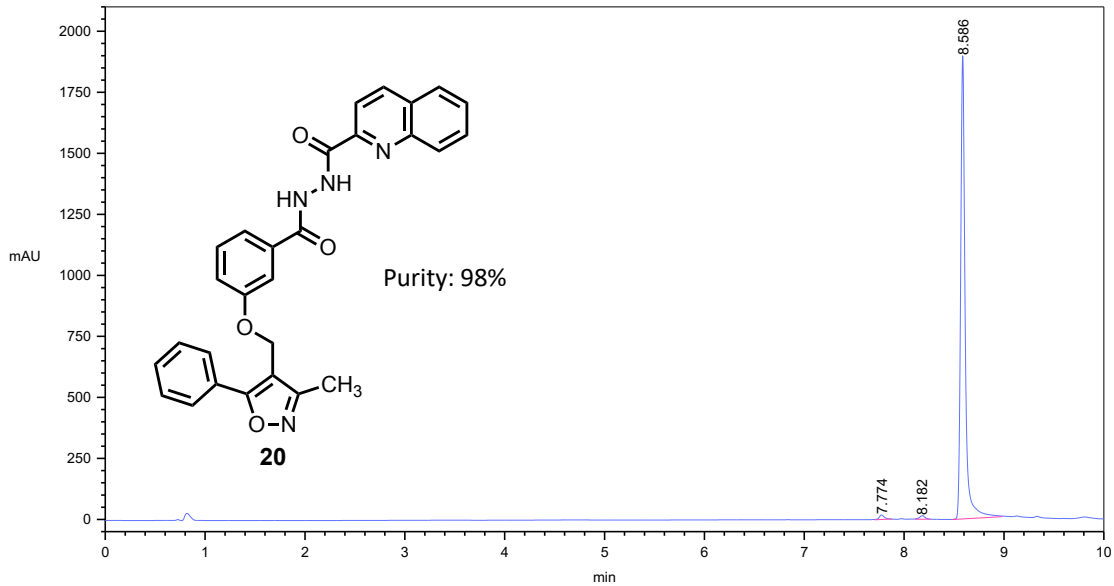

Peak	RetTime (min)	Area (mAU*s)	Height (mAU)	Area (%)
1	7.774	68.82444	19.65042	1.1907
2	8.182	36.59236	12.5091	0.6331
3	8.586	5674.78396	1884.62500	98.1762

21

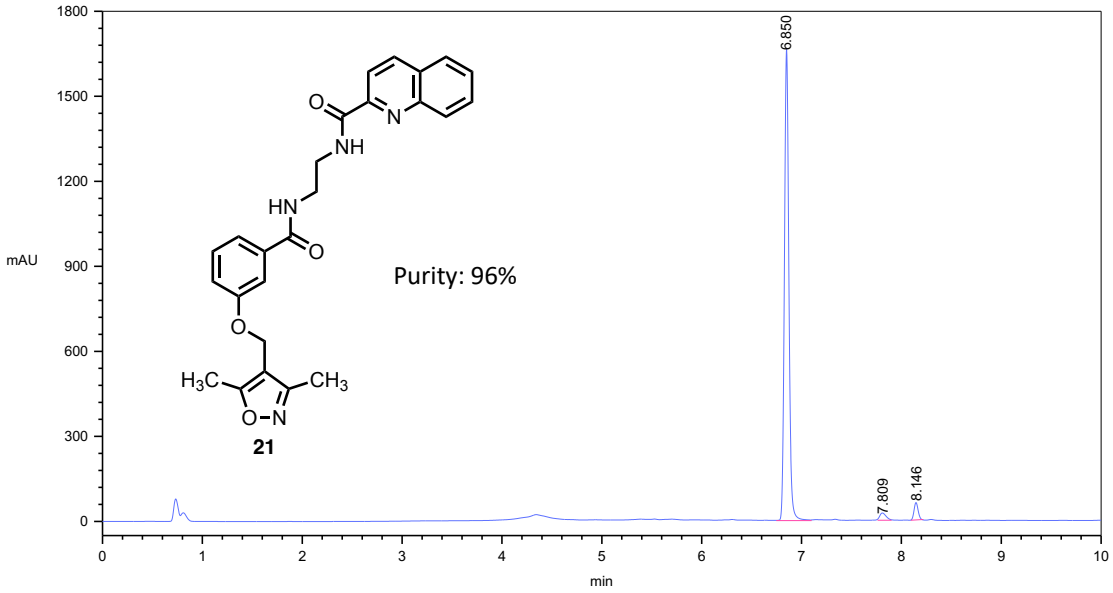

Peak	RetTime (min)	Area (mAU*s)	Height (mAU)	Area (%)
1	6.850	5141.86963	1663.25903	95.7817
2	7.809	103.18970	24.77596	1.9222
3	8.146	123.25990	52.21564	2.2961

22

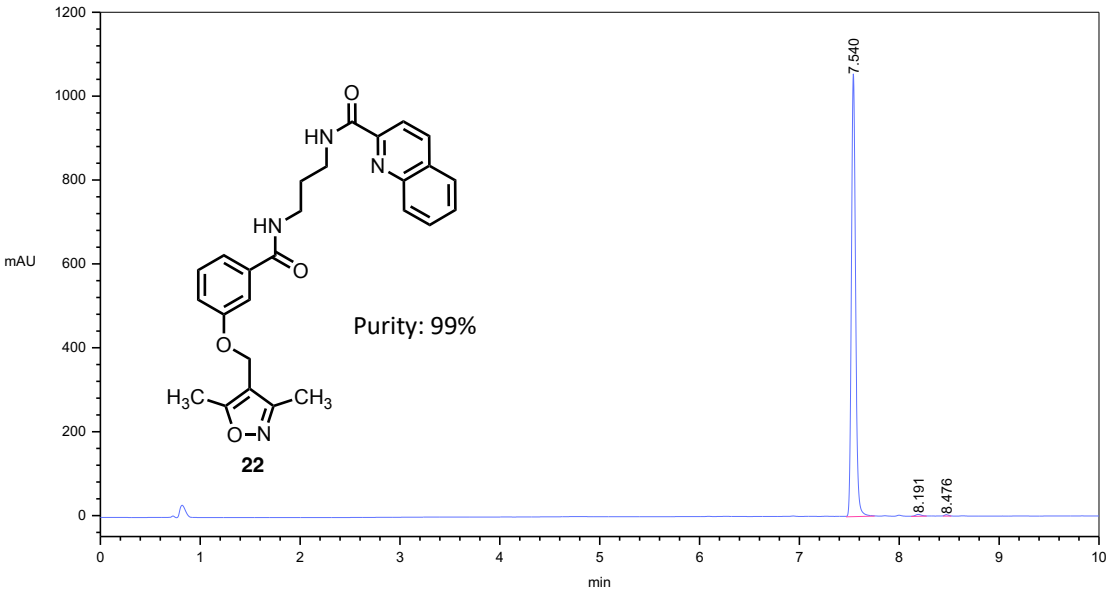

Peak	RetTime (min)	Area (mAU*s)	Height (mAU)	Area (%)
1	7.540	3082.96973	1058.75903	99.0332
2	8.191	21.18954	5.18325	0.6807
3	8.476	8.90759	3.50440	0.2861

23

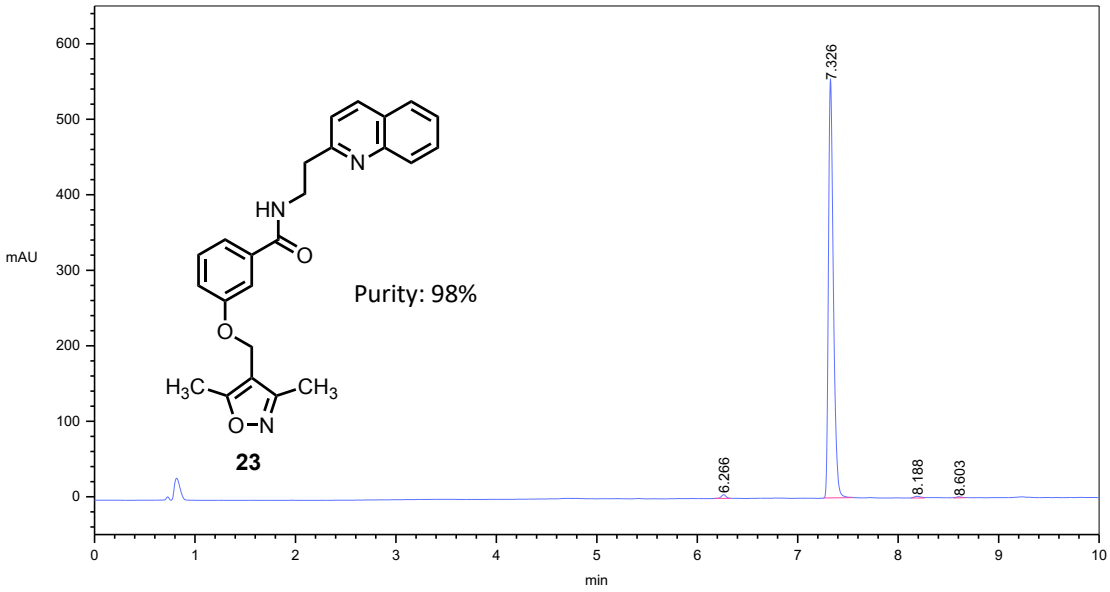

Peak	RetTime (min)	Area (mAU*s)	Height (mAU)	Area (%)
1	6.266	12.41452	4.17340	0.6486
2	7.326	1871.71509	554.90857	97.7936
3	8.188	23.82956	4.61825	1.2451
4	8.603	5.98485	1.58921	0.3127

24

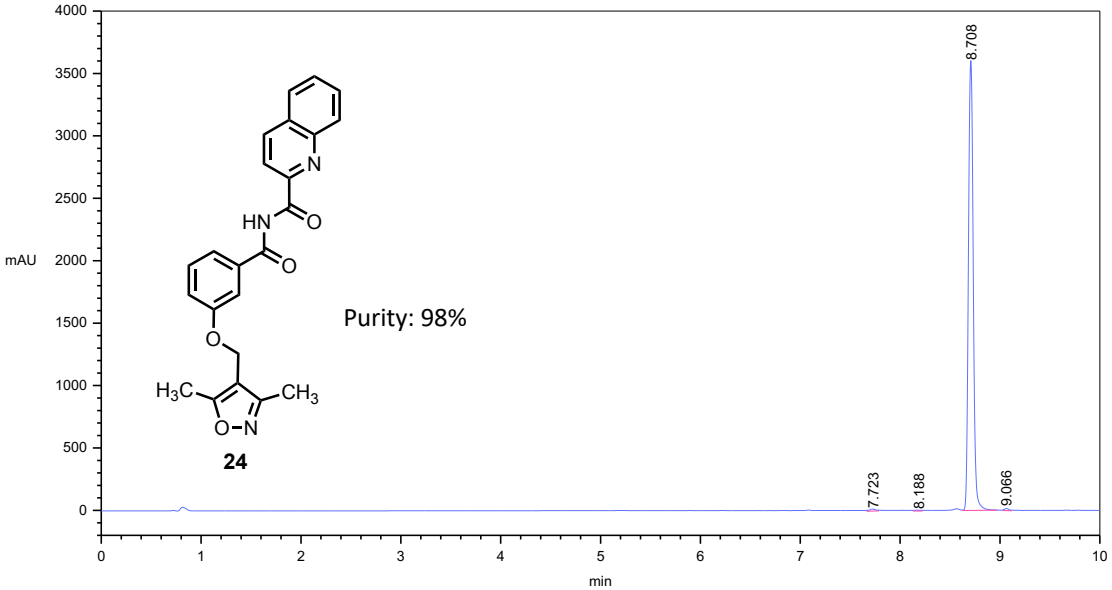

Peak	RetTime (min)	Area (mAU*s)	Height (mAU)	Area (%)
1	7.723	81.48239	18.74687	0.6777
2	8.188	58.59719	27.54438	0.4874
3	8.708	1.18029e4	3591.81396	98.1718
4	9.066	79.71532	20.06610	0.6630

25

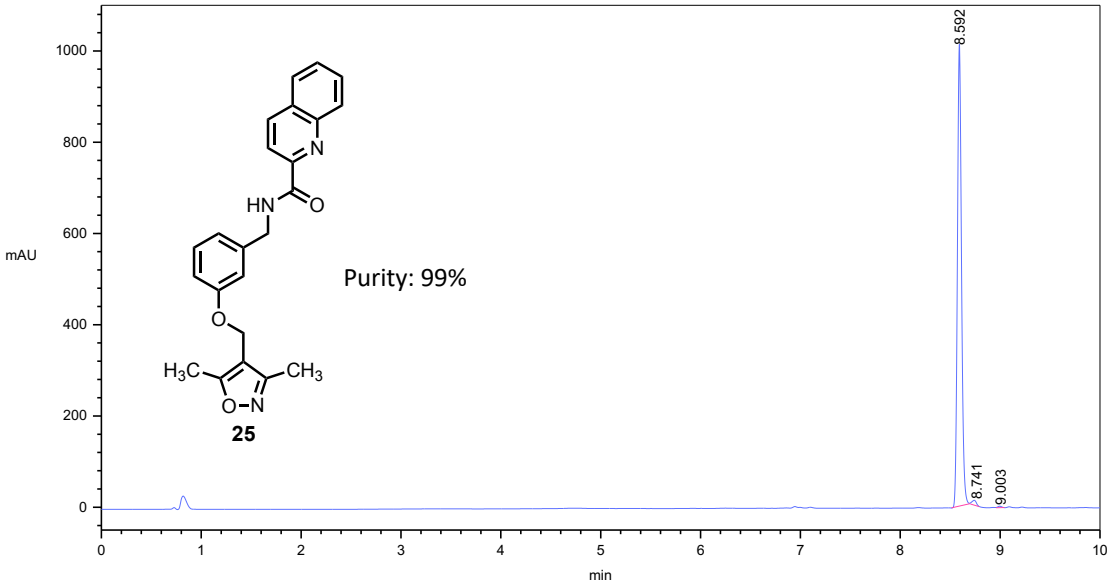

Peak	RetTime (min)	Area (mAU*s)	Height (mAU)	Area (%)
1	8.592	2928.38403	1014.54187	98.5218
2	8.741	32.66558	11.09223	1.0990
3	9.003	11.27080	3.53641	0.3792

26

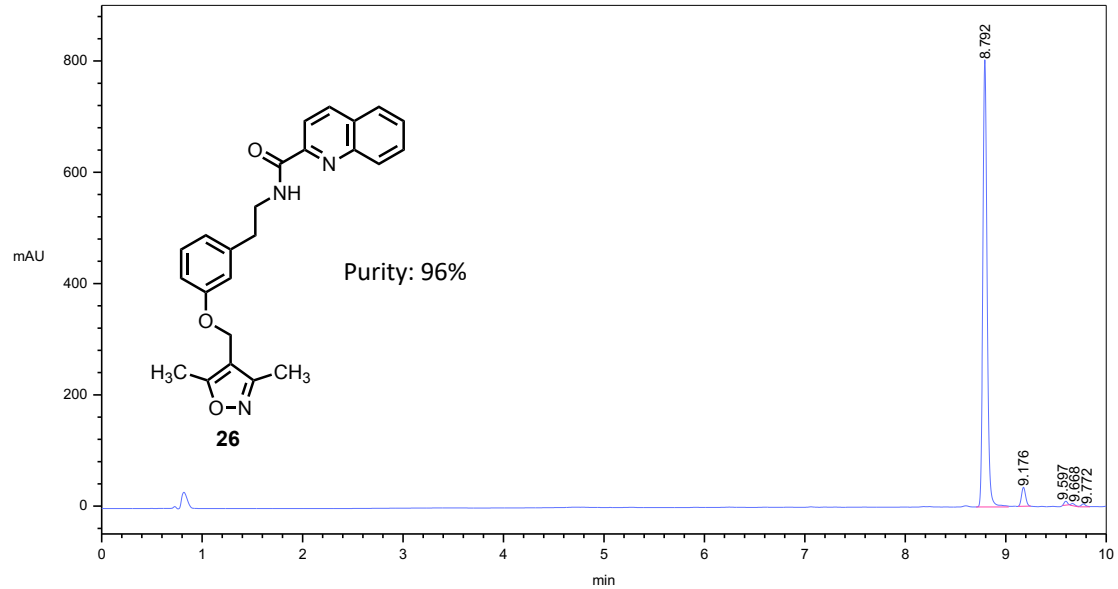

Peak	RetTime (min)	Area (mAU*s)	Height (mAU)	Area (%)
1	8.792	2348.19849	803.76880	96.1476
2	9.176	67.99582	28.84383	2.7841
3	9.597	14.46004	6.67765	0.5921
4	9.668	3.25859	1.98490	0.1334
5	9.772	8.37283	3.79583	0.3428